Apportionment of PM10 sources in the Richmond airshed, Tasman District

T. Ancelet P.K. Davy

GNS Science Consultancy Report 2016/49
January 2017 Amended FINAL

Apportionment of PM_{10} sources in the Richmond airshed, Tasman District

T. Ancelet P.K. Davy

GNS Science Consultancy Report 2016/49
January 2017 Amended FINAL

DISCLAIMER

This report has been prepared by the Institute of Geological and Nuclear Sciences Limited (GNS Science) exclusively for and under contract to Tasman District Council. Unless otherwise agreed in writing by GNS Science, GNS Science accepts no responsibility for any use of or reliance on any contents of this report by any person other than Tasman District Council and shall not be liable to any person other than Tasman District Council, on any ground, for any loss, damage or expense arising from such use or reliance.

Use of Data:

Date that GNS Science can use associated data: May 2016

BIBLIOGRAPHIC REFERENCE

Ancelet, T.; Davy, P.K. 2016. Apportionment of PM_{10} sources in the Richmond airshed, Tasman District, *GNS Science Consultancy Report* 2016/49. 49 p.

CONTENTS

FIGURES

TABLES

APPENDICES

APPENDIX FIGURES

EXECUTIVE SUMMARY

This report presents the results of an analysis of particulate matter (PM_{10}) concentrations and composition in Tasman District Council's Richmond airshed. The compositional data has been used in a receptor modelling study to apportion particulate matter emission sources contributing to ambient PM_{10} concentrations in the airshed.

Key results from the study are:

1. Emissions from biomass combustion, attributed to solid fuel fires for home heating during the winter, were the primary source of PM_{10} in the Richmond airshed and were also the dominant source contributing to exceedances of the PM_{10} National Environmental Standard for Air Quality (NES) of 50 $\mu g\ m^{-3}$.
2. Based on studies elsewhere in New Zealand where home heating is responsible for high pollution nights during winter, most of the particulate matter is in the fine fraction ($PM_{2.5}$) and therefore it was likely that there were more days where $PM_{2.5}$ exceeded the New Zealand Ambient Air Quality Guidelines (NZAAQG) of 25 $\mu g\ m^{-3}$ compared to PM_{10} NES exceedances.
3. It was found that annual average arsenic concentrations for 2014 at Richmond (14 ng m^{-3}) exceeded the New Zealand Ambient Air Quality Guideline value of 5.5 ng m^{-3} (annual average). Elemental arsenic and lead in particulate matter were found to be strongly associated with the biomass combustion source with peaks in concentrations during winter. The arsenic and lead contamination was considered to be from the use of copper chrome arsenate (CCA) treated timber and old painted timber respectively as fuel for domestic fires. A second source of arsenic in PM_{10} was also identified and considered to be separate from that associated with domestic solid fuel fires.

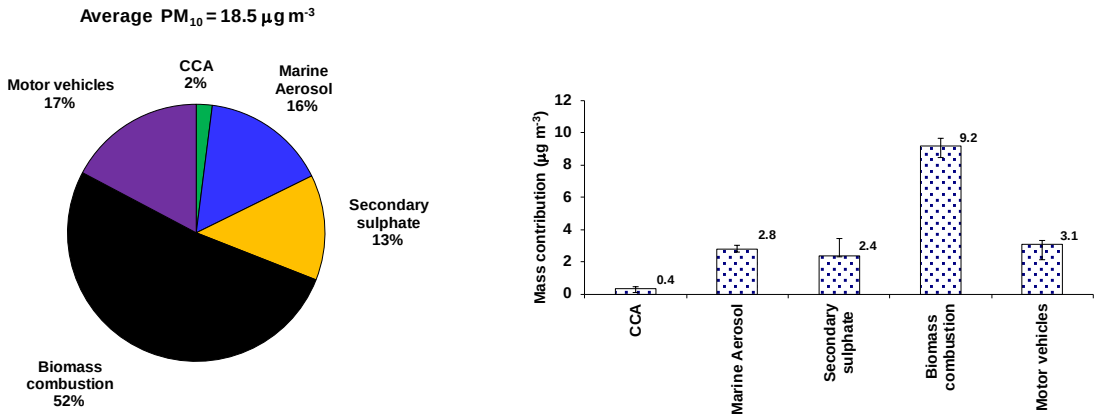

Figure ES1 Average source contributions to PM_{10} in Richmond over the monitoring period (June 2013 – September 2015).

1.0 INTRODUCTION

This report presents results from an investigation of PM_{10} sources measured at an ambient air quality monitoring site in Richmond, Tasman District. In Richmond, PM_{10} concentrations exceeding the National Environmental Standard for Air Quality (NES) of 50 µg/m^3 occur regularly during the winter months. While Tasman District Council has undertaken an emissions inventory for this area, there are significant uncertainties in the estimates because emissions inventories can only assess anthropogenic discharges, are not able to reliably estimate contributions from sources such as wind-blown dusts or sea spray, effects of meteorology, and do not take into account the impact of emissions occurring from outside the airshed, such as on the Waimea Plains or in the adjoining Nelson City Council area or arising from aircraft or shipping. This work was commissioned by Tasman District Council (TDC) as part of their ambient air quality monitoring strategy and was partly funded by an Envirolink grant (1604-TSDC117) from the Ministry of Business, Innovation and Employment.

1.1 REQUIREMENT TO MANAGE AIRBORNE PARTICLE POLLUTION

In response to growing evidence of significant health effects associated with airborne particle pollution, the New Zealand Government introduced a National Environmental Standard (NES) in 2005 of 50 µg m^{-3} for particles less than 10 µm in aerodynamic diameter (denoted as PM_{10}). The NES places an onus on regional councils to monitor PM_{10} and publicly report if the air quality in their region exceeds the standard. Initially, regional councils were required to comply with the standard by 2013 or face restrictions on the granting of resource consents for discharges that contain PM_{10}, but the NES has since been revised, extending the target date for regional councils to comply with the standard. The new target dates are September 1, 2016 for airsheds with between 1 and 10 exceedances and September 1, 2020 for airsheds with 10 or more exceedances. In areas where the PM_{10} standard is exceeded, information on the sources contributing to those air pollution episodes is required to effectively manage air quality and formulate appropriate mitigation strategies.

1.2 IDENTIFYING THE SOURCES OF AIRBORNE PARTICLE POLLUTION

Measuring the mass concentration of particulate matter (PM) provides little or no information on the identities of the contributing sources. Airborne particles are composed of many elements and compounds emitted from various sources and a multivariate analysis technique known as receptor modelling allows the determination of relative mass contributions from sources impacting the total PM mass of samples collected at a monitoring site. First, gravimetric mass is measured and then a variety of methods can be used to determine the elements and compounds present in a sample. In this study, elemental concentrations in the samples were determined using X-ray fluorescence spectroscopy (XRF) at GNS Science in Lower Hutt.

X-ray fluorescence is a mature analytical technique that provides the non-destructive determination of multi-elemental concentrations in samples. Using elemental concentrations, coupled with appropriate statistical techniques and purpose-designed mathematical models, the sources contributing to each ambient sample can be identified. In general, the more ambient samples that are included in the analysis, the more robust the receptor modelling results. Appendix 1 provides a description of the XRF analytical process and receptor modelling techniques.

1.3 REPORT STRUCTURE

This report is comprised of 5 main chapters. The remaining chapters have been broken down as follows:

1. Chapter 2 describes the methodology and analytical techniques used for the receptor modeling analysis.
2. Chapter 3 describes the Richmond ambient air quality monitoring site, temporal trends in PM_{10} concentrations and local meteorology.
3. Chapter 4 presents the receptor modeling results for PM_{10}, including temporal variations and seasonality.
4. Chapter 5 presents a discussion of the receptor modeling results.

2.0 METHODOLOGY

PM_{10} samples were collected onto Teflon filters using a Partisol sampler located at 56 Oxford Street in Richmond. Figure 2.1 presents the location of the monitoring site. In addition to the Partisol sampler, the monitoring site also featured an FH62 beta attenuation monitor (BAM) measuring PM_{10} concentrations continuously and a meteorological station collecting parameters such as wind speed and direction and ambient temperature. All PM sampling and systems maintenance at the sampling site was carried out by TDC, and as such, TDC maintains all records of equipment, flow rates and sampling methodologies used for the PM sampling regimes. Filter conditioning, weighing and re-weighing for PM_{10} gravimetric mass determinations were carried out by Watercare Services Limited.

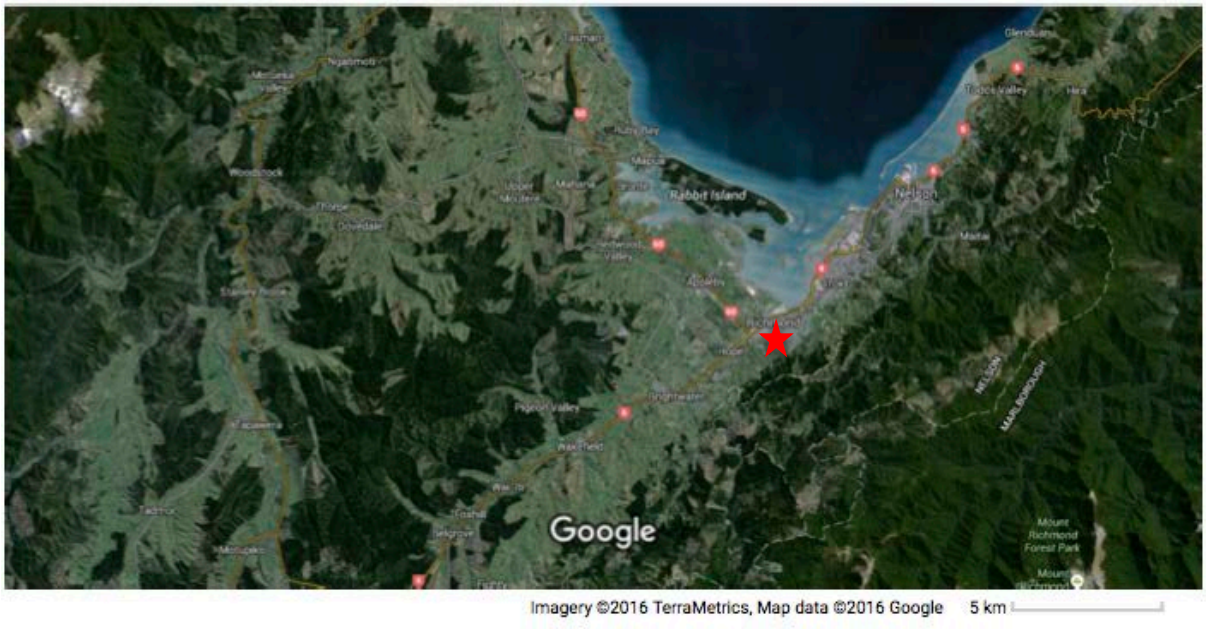

Figure 2.1 Location of the Oxford Street monitoring site in Richmond (★) (source: Google Maps).

Elemental concentrations in PM_{10} were determined using X-ray fluorescence spectroscopy (XRF) at the New Zealand Ion Beam Analysis Facility in Gracefield, Lower Hutt. Black carbon (BC) concentrations were determined using light reflection techniques. Full descriptions of the analytical techniques used in this study are provided in Appendix 1.

The authors have been provided with information about the monitoring site and have been informed of the typical activities in the surrounding areas that may contribute to PM_{10} concentrations. These details informed the conceptual receptor model described in Chapter 3.

2.1 DATA ANALYSIS AND REPORTING

The receptor modelling results within this report have been produced in a manner that provides as much information as possible on the relative contributions of sources to PM concentrations so that it may be used for monitoring strategies, air quality management and policy development. The data have been analysed to provide the following outputs:

1. masses of elemental species apportioned to each source;
2. source elemental profiles;
3. average PM_{10} mass apportioned to each source;

4. temporal variations in source mass contributions (timeseries plots);
5. seasonal variations in source mass contributions. For the purposes of this study, summer has been defined as December–February, autumn as March–May, winter as June–August and spring as September–November;
6. analysis of source contributions on peak PM days.

Table 2.1 presents the relevant standards, guidelines and targets for PM concentrations.

Table 2.1 Standards, guidelines and targets for PM concentrations

Particle Size	Averaging Time	Ambient Air Quality Guideline	MfE* 'Acceptable' air quality category	National Environmental Standard
PM_{10}	24 hours	50 µg m^{-3}	33 µg m^{-3}	50 µg m^{-3}
	Annual	20 µg m^{-3}	13 µg m^{-3}	
$PM_{2.5}$	24 hours	25 µg m^{-3}	17 µg m^{-3}	

*Ministry for the Environment air quality categories taken from the Ministry for the Environment, October 1997 – ***Environmental Performance Indicators: Proposals for Air, Fresh Water and Land***.

3.0 OXFORD STREET MONITORING SITE AND SAMPLING METHODOLOGY

3.1 SITE DESCRIPTION

PM_{10} samples were collected at an ambient air quality monitoring station located at 56 Oxford street, Richmond (Lat: 41°20'21.46 S; Long: 173°10'58.65 E; elevation: 13 m). Figure 3.1 presents the site location on a map of the local area.

Figure 3.1 Map showing the location of the Oxford Street monitoring site (source: TDC).

Oxford Street is located near the Richmond CBD and the monitoring site was less than 400 m from State Highway 6, the major roadway into and out of Nelson. The site was in a residential area and was surrounded by buildings no higher than two stories. Aside from its immediate environment, the monitoring site was surrounded by hills and farmland, and was less than 5 km south of Tasman Bay.

3.2 PARTICULATE MATTER SAMPLING AND MONITORING PERIOD

In this study, 256 PM_{10} samples were collected between June 2013 and mid-September 2015 using a Partisol sampler. Generally, samples were collected on a one-day-in-three (midnight to midnight) sampling regime, although samples collected during the winter were collected on a one-day-in-two sampling regime. Mass concentrations of PM_{10} and $PM_{2.5}$ were determined gravimetrically, where a filter of known weight was used to collect the PM samples from a known volume of sampled air. The loaded filters were then re-weighed to obtain the mass of collected PM. The average PM concentration in the sampled air was then calculated.

3.3 CONCEPTUAL RECEPTOR MODEL FOR PM_{10} IN RICHMOND

An important part of the receptor modeling process is to formulate a conceptual model of the receptor site. This means understanding and identifying the major sources that may influence ambient PM concentrations at the site. For the Richmond site, the initial conceptual model includes local emission sources:

- Motor vehicles – all roads in the area act as line sources, and roads with higher traffic densities and congestion will dominate;
- Domestic activities – likely to be dominated by biomass combustion activities like emissions from solid fuel fires used for domestic heating during the winter;
- Local wind-blown soil or road dust sources may also contribute.

Sources that originate further from the monitoring site would also be expected to contribute to ambient particle loadings, and these include:

- Marine aerosol;
- Secondary PM resulting from atmospheric gas-to-particle conversion processes – includes sulphates, nitrates and organic species;
- Potential industrial emissions from combustion processes (boilers) and dust generating activities;
- Emissions from ships in the Port area of Nelson.

Another category of emission sources that may contribute are those considered to be 'one-off' emission sources:

- Fireworks displays and other special events (e.g. Guy Fawkes day);
- Short-term road works and demolition/construction activities.

The variety of sources described above can be recognised and accounted for using appropriate data analysis methods such as examination of seasonal differences, temporal variations and receptor modeling itself.

3.4 LOCAL METEOROLOGY IN RICHMOND

A meteorological station was located on the roof of the Tasman District Council (TDC) building at 189 Queen Street approximately 300 m from the PM monitoring site. The meteorological station is owned and operated by TDC. As shown in Figure 3.2, the predominant wind directions were from the southwest and north/northeast. Winds from other directions were uncommon. Some seasonality was apparent in wind speeds, with speeds lower during winter, but no seasonality was apparent for wind directions (Figure 3.3).

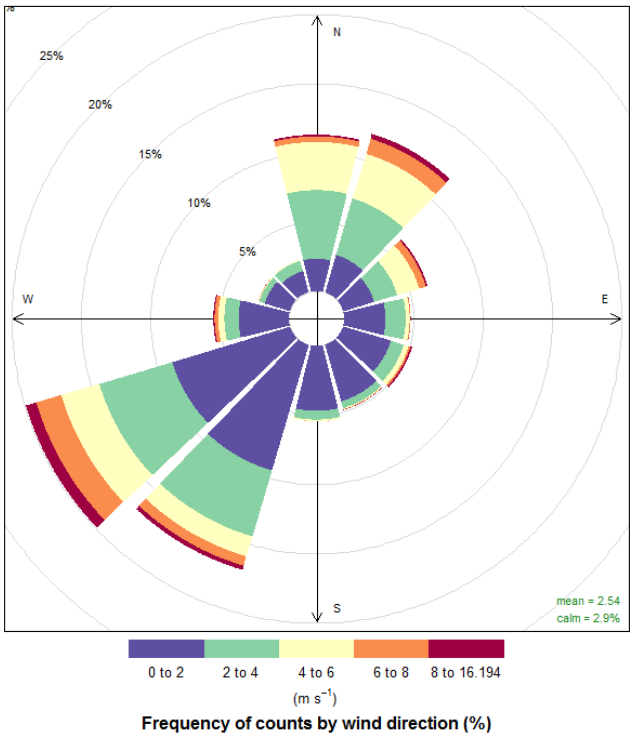

Figure 3.2 Wind rose for the entire monitoring period (June 2013 – September 2015).

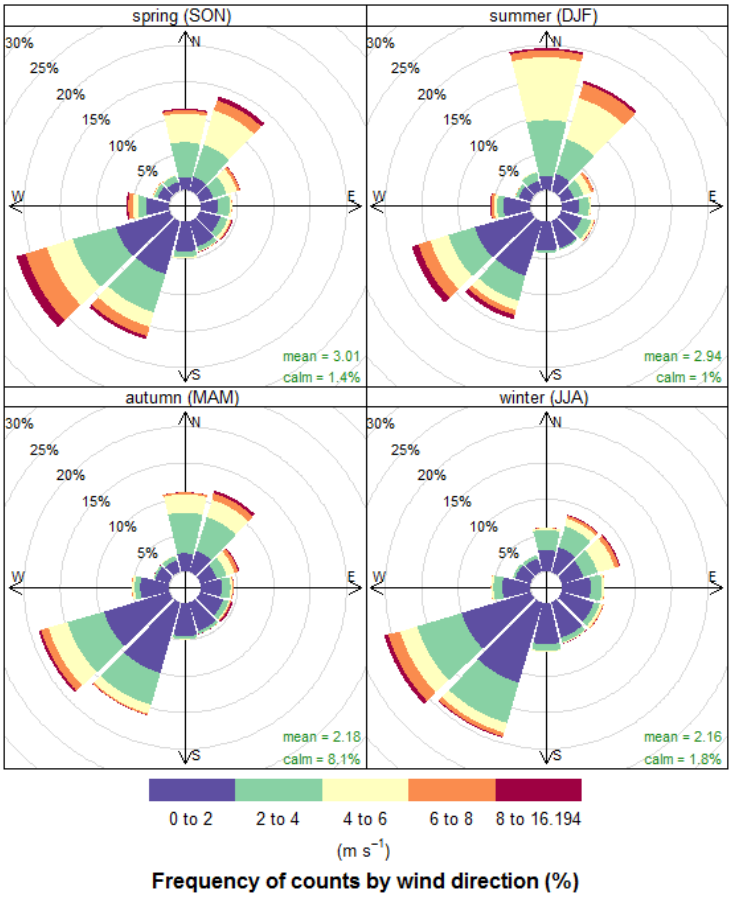

Figure 3.3 Wind roses by season over the entire monitoring period (June 2013 – September 2015).

3.5 PM_{10} CONCENTRATIONS IN RICHMOND

PM_{10} concentrations were continuously monitored at the Richmond site using a Thermo-Anderson FH62 Beta-particle Attenuation Monitor (BAM) operated according to AS/NZS 3580.9.11.2008. Figure 3.4 presents the BAM PM_{10} monitoring results (midnight to midnight) over the monitoring period (June 2013–October 2015). Figure 3.4 shows that PM_{10} concentrations in Richmond have seasonal patterns, with concentrations peaking during winter. Gaps present in Figure 3.4 are from sampler malfunction/maintenance. Between 2013 and 2015, the NES was exceeded eleven times (http://www.tasman.govt.nz/environment/air/air-quality/).

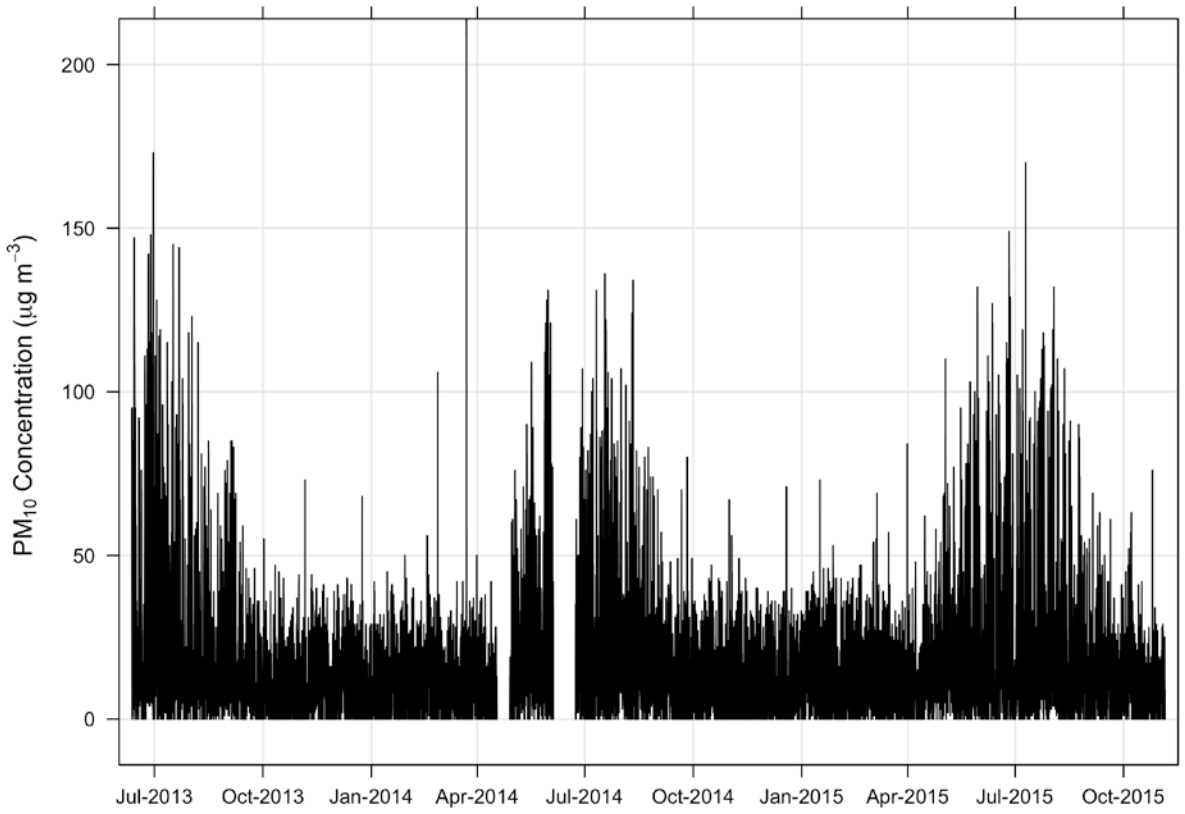

Figure 3.4 PM_{10} (BAM) concentrations in Richmond (data supplied by TDC).

4.0 RECEPTOR MODELING ANALYSIS OF PM_{10} IN RICHMOND

4.1 ANALYSIS OF PM_{10} SAMPLES COLLECTED

PM_{10} samples in Richmond were collected using a Partisol sampler system, typically on a one-day-in-three sampling regime, although samples collected during the winter were collected on a one-day-in-two regime. Overall, 256 samples were collected from June 2013 to September 2015. PM_{10} concentrations were determined gravimetrically and elemental and BC concentrations were determined using XRF and light reflection, respectively, as described in Appendix 1. Gravimetric results for the PM_{10} samples are presented in Figure 4.1. Clear seasonal patterns are apparent from Figure 4.1, with PM_{10} concentrations peaking from May–August. Outside of the winter season, PM_{10} concentrations were low. Gaps present in Figure 4.1 resulted from missed sample days or samples removed as part of the quality assurance process, which could include, but would not be limited to, samples being collected on the wrong side of the filter, double exposure of filters, no volumetric data available, or equipment failure.

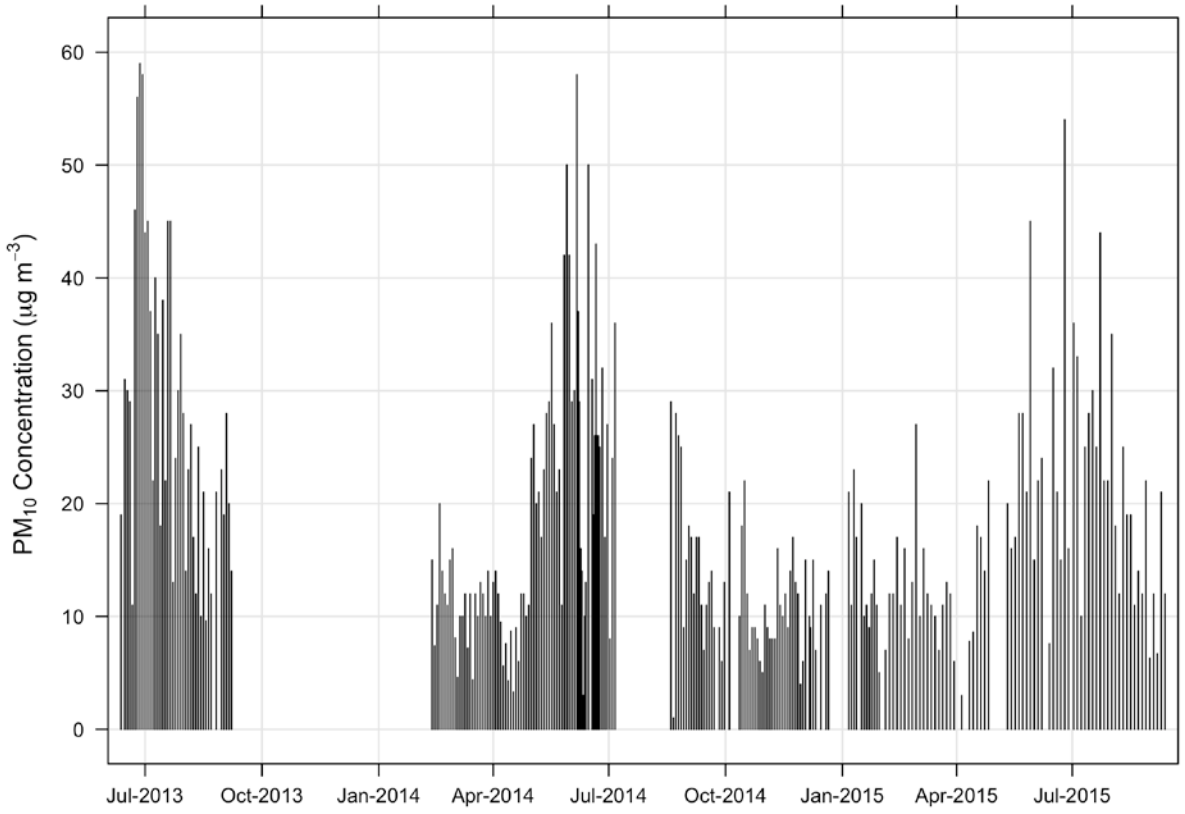

Figure 4.1 Gravimetric PM_{10} results. Gaps are from missed sample days or samples removed as part of the quality assurance process.

4.2 COMPOSITION OF PM_{10}

Elemental concentrations in the samples collected are presented in Table 4.1. Table 4.1 indicates that some measured species were close to or below their respective limit of detection (LOD) in each of the samples. Carbonaceous species, represented by BC, were found to dominate PM_{10} mass concentrations. Along with BC, other important elemental constituents included Na, Cl, Si, Al and S, indicating that combustion sources, marine aerosol, crustal matter and secondary sulphate particles are important contributors to PM_{10} concentrations at the monitoring site. An elemental correlation plot is provided in Figure A2.1 in Appendix 2.

Table 4.1 Elemental concentrations in PM_{10} samples from Richmond (256 samples).

	Ave (ng m^{-3})	Median (ng m^{-3})	Max (ng m^{-3})	Min (ng m^{-3})	Std Dev (ng m^{-3})	Ave Uncert (ng m^{-3})	# > LOD	% > LOD
PM_{10} (µg m^{-3})	19	15	59	1	12			
BC	3997	3193	12665	297	3314	297	256	100
Na	704	530	3557	22	612	116	247	96
Mg	177	172	529	0	95	19	254	99
Al	146	114	911	0	165	22	153	60
Si	434	343	1717	0	337	51	254	99
P	6	0	91	0	15	7	42	16
S	207	186	829	0	186	27	199	78
Cl	977	521	7234	13	1176	100	256	100
K	283	222	969	43	190	30	256	100
Ca	182	157	636	3	111	20	256	100
Ti	16	13	64	0	12	3	240	94
V	1	0	8	0	1	1	68	27
Cr	11	1	190	0	27	2	144	56
Mn	7	7	20	0	4	1	247	96
Fe	188	152	659	10	128	20	256	100
Co	0.4	0	3	0	1	3	0	0
Ni	1	0	5	0	1	1	64	25
Cu	10	3	125	0	20	2	181	71
Zn	17	11	107	0	16	3	239	93
Ga	1	0	6	0	1	7	0	0
As	16	9	137	0	21	2	219	86
Se	0	0	7	0	1	10	0	0
Br	10	6	83	0	12	7	126	49
Sr	2	1	11	0	2	5	18	7
Y	1	0	5	0	1	6	0	0
Zr	1	0	13	0	3	9	2	1
Nb	3	2	11	0	3	9	5	2
Mo	2	1	10	0	2	10	0	0
Pd	2	0	14	0	3	5	43	17
Cd	2	0	16	0	3	7	21	8
Sn	4	3	23	0	5	8	47	18
Sb	7	6	34	0	6	8	102	40
Te	4	0	29	0	6	9	38	15
Cs	10	8	77	0	11	10	111	43
Ba	7	0	64	0	11	9	64	25
Pb	18	16	61	0	12	3	243	95

Table 4.1 also shows that some of the heavy metal elements are present at significant concentrations above their respective LOD, particularly for arsenic and lead. Figure 4.2 presents the temporal variation for arsenic and lead showing a winter peak for both contaminants. Interestingly arsenic concentrations also had some significant non-winter peaks. When examined in conjunction with the elemental correlation plot in Appendix 2 it shows that arsenic and lead concentrations are correlated with black carbon suggesting that they are associated with combustion sources.

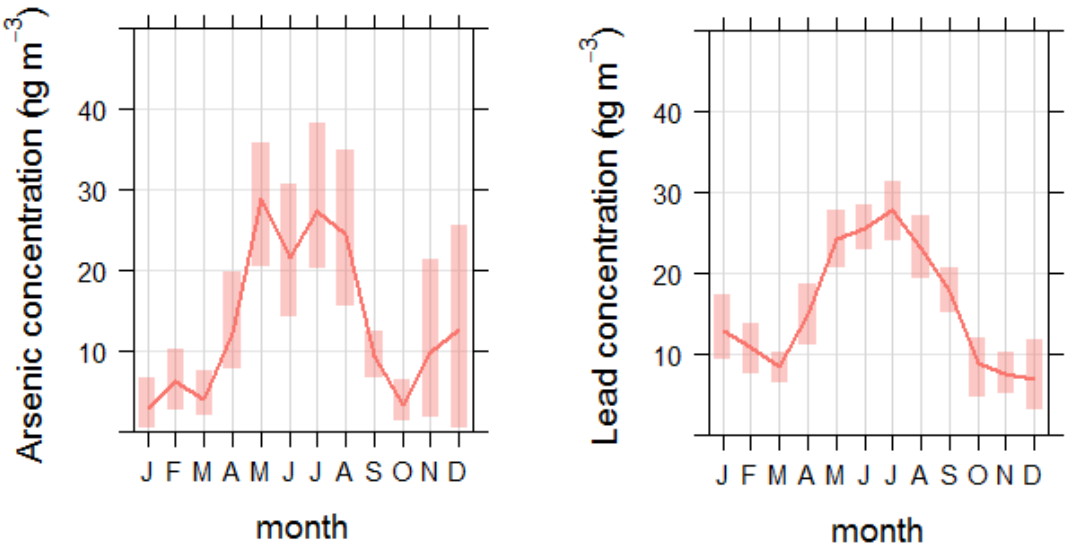

Figure 4.2 Temporal variation for arsenic (left); and lead (right) showing peak winter concentrations. Shaded areas represent the 95% confidence intervals.

The New Zealand ambient air quality guidelines (AAQG) provide guideline values for arsenic (inorganic arsenic is 5.5 ng m^{-3} as an annual average) and lead (200 ng m^{-3} as a 3-month moving average, calculated monthly) in PM_{10} (MfE 2002). The calculation of an annual average for arsenic from the Richmond data was possible for 2014 since this is the only year that monitoring covered the entire period. For 2014, the annual average arsenic concentration was 14 ng m^{-3}, nearly three times the AAQG value. Table 4.1 indicates that the long term average for arsenic is of a similar value (16 ng m^{-3}). The 3-month moving average lead concentrations peaked during winter at around 25-30 ng m^{-3}, somewhat less than the AAQG of 200 ng m^{-3}.

4.3 SOURCE CONTRIBUTIONS TO PM_{10} IN RICHMOND

Five source contributors were identified from PMF receptor modeling analysis of the PM_{10} data from Richmond. Table 4.2 and Figure 4.3 present the source profiles extracted from the PMF analysis. The source contributors identified were found to explain 96% of the gravimetric PM_{10} mass on average.

The sources identified were:

- Biomass combustion: The first factor was identified as biomass combustion based on the dominance of BC and K in the profile (Fine, Cass et al. 2001, Khalil and Rasmussen 2003). Arsenic and lead were strongly associated with the biomass combustion profile. This phenomenon is consistent throughout New Zealand and indicates that residents are burning copper chrome arsenate-treated and lead-painted timber, respectively (Ancelet et al. 2012);

- Marine aerosol: the second factor was identified as a marine aerosol source because of the predominance of Na and Cl, along with some Mg, S, K, and Ca;
- Secondary sulphate: the third factor was identified as sulphate because of the dominance of sulphur in the profile. This source contribution was from secondary sulphate aerosol produced in the atmosphere from gaseous precursors;
- Motor vehicles: the fourth factor was identified as motor vehicles because of the presence of BC, Si, Ca, Ti and Fe as significant elemental components. This profile is likely a combination of tailpipe (BC representing fuel combustion) and re-entrained road dust emissions (Si, Ca, Ti, Fe as the crustal matter components);
- CCA: the fifth factor was identified as originating from emissions of copper chrome arsenate containing particulate matter. This is the first time a CCA profile has been extracted from speciation data in New Zealand

Table 4.2 Source elemental concentration profiles for PM_{10} samples from Richmond.

	Biomass combustion (ng m^{-3})	**Marine aerosol (ng m^{-3})**	**Secondary sulphate (ng m^{-3})**	**Motor vehicles (ng m^{-3})**	**CCA (ng m^{-3})**
PM_{10}	9177	2783	2350	3057	355
BC	3254.2	15.1	225.2	397.9	62.7
Na	16.0	500.3	117.9	32.7	21.6
Mg	6.8	92.2	47.6	16.2	7.8
Si	37.9	9.6	45.7	329.3	0.0
S	16.8	0.0	169.4	7.0	0.3
Cl	36.0	764.7	13.0	53.3	33.2
K	152.6	28.0	29.0	51.1	7.9
Ca	20.9	25.2	17.5	106.2	5.1
Ti	2.3	0.6	1.0	10.9	0.2
Cr	0.0	0.1	0.9	0.0	10.0
Mn	1.3	0.5	1.0	2.9	0.3
Fe	38.6	8.0	17.7	120.1	0.4
Cu	1.3	0.2	0.0	0.9	5.4
Zn	11.1	0.0	0.6	2.7	0.4
As	6.9	0.0	0.7	0.2	6.4
Pb	10.5	1.6	0.9	1.6	0.8

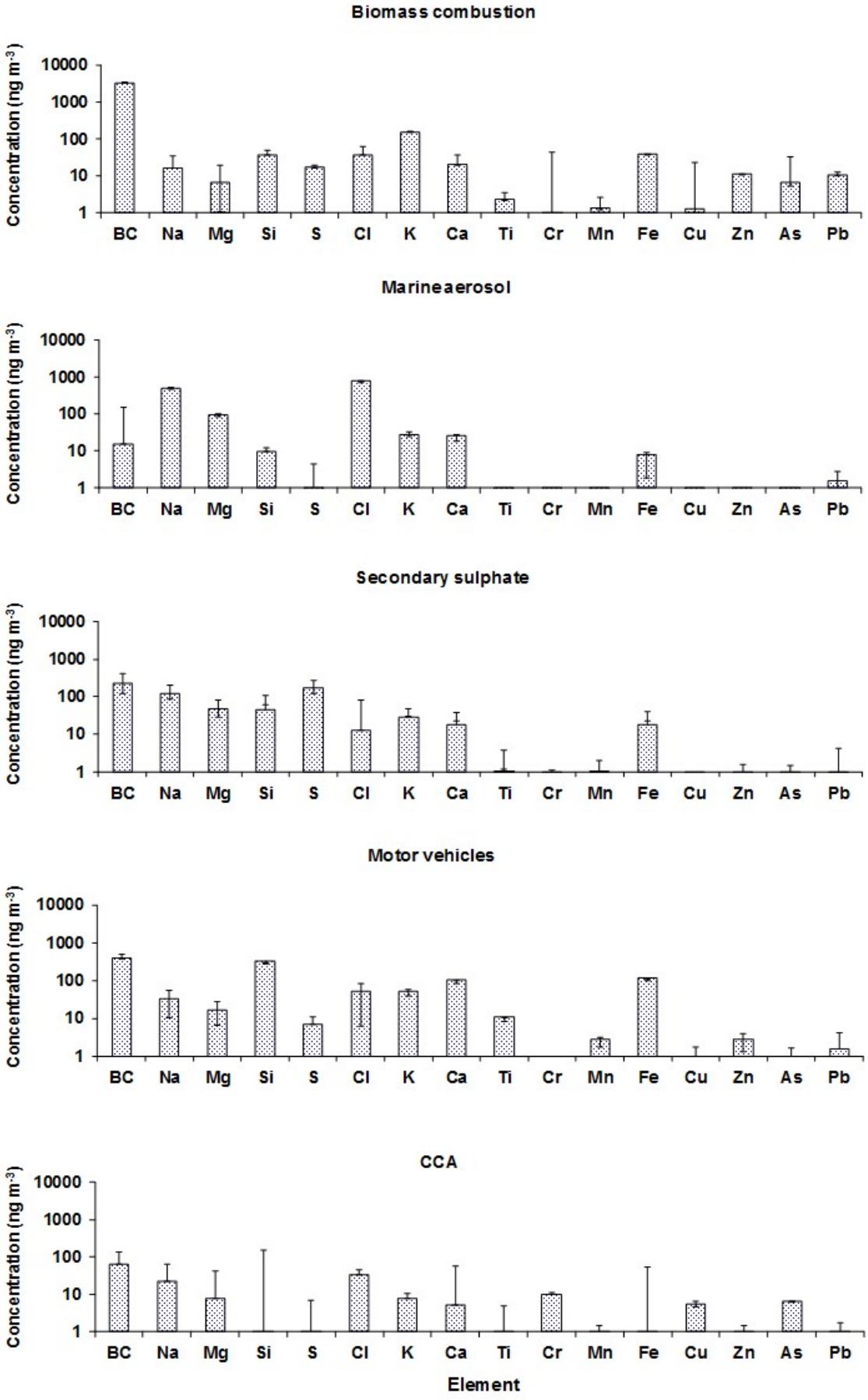

Figure 4.3 Source elemental concentration profiles for PM_{10} samples from Richmond.

Figure 4.4 presents the relative source contributions to PM_{10} in Richmond. Also included in the Figure 4.4 are the 5th and 95th percentile confidence limits in mass contributions for each of the sources, indicating the variability in average mass contributions over the monitoring period.

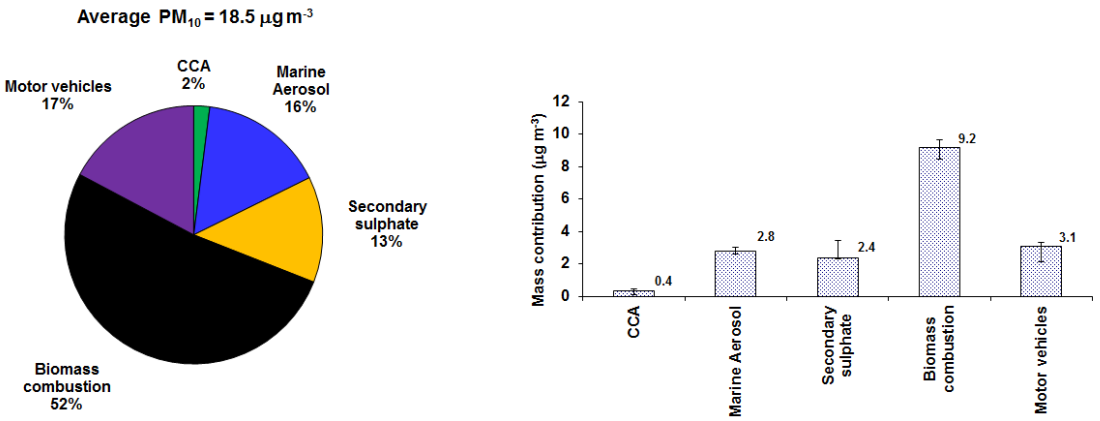

Figure 4.4 Average source contributions to PM_{10} in Richmond over the monitoring period (June 2013 – September 2015).

The average PM_{10} source contributions over the entire monitoring period estimated from the PMF analysis showed that biomass combustion was the most significant contributor to PM_{10} mass (52%). Secondary sulphate (13%), marine aerosol (16%) and motor vehicles (17%) had similar contributions to PM_{10} mass, while CCA had the lowest (trace) contribution (2%). The calculation of annual average source contributions was only possible for 2014 due to missing data (<75 % representative data coverage) during 2013 and 2015. Figure 4.5 presents the annual average source contributions for 2014.

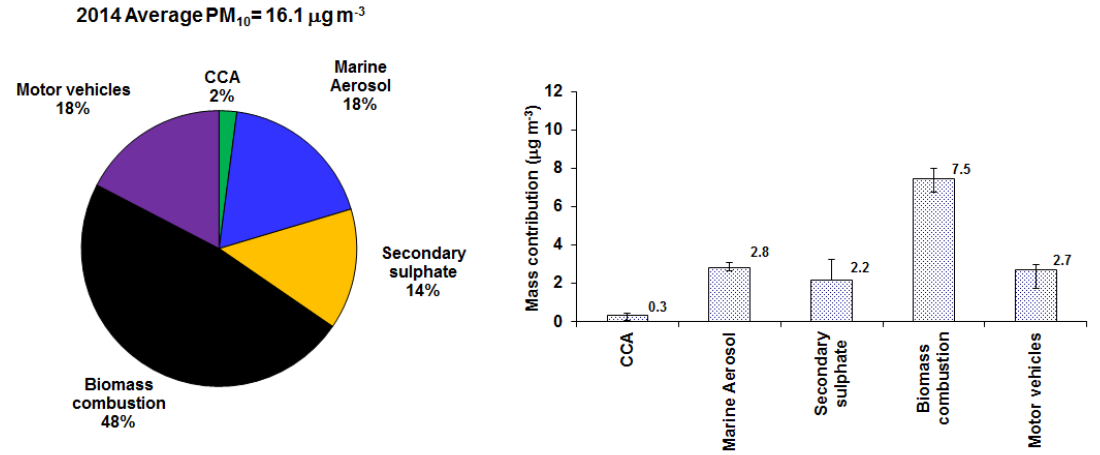

Figure 4.5 Annual (2014) average source contributions to PM_{10} in Richmond.

The relative source contributions to the 2014 annual average as presented in Figure 4.5 were similar to the longer term averages over the entire monitoring period and were dominated by the biomass burning source.

Temporal variations in the source contributions are presented in Figure 4.6 (note that gaps in the data are due to missing sample periods). It was evident that PM mass is dominated by the biomass combustion source during winter, which arises primarily from emissions from

solid fuel fires used for domestic heating. During other time periods, marine aerosol, sulphate and motor vehicle contributions can be significant. The PM due to the CCA source was present intermittently at relatively low concentrations.

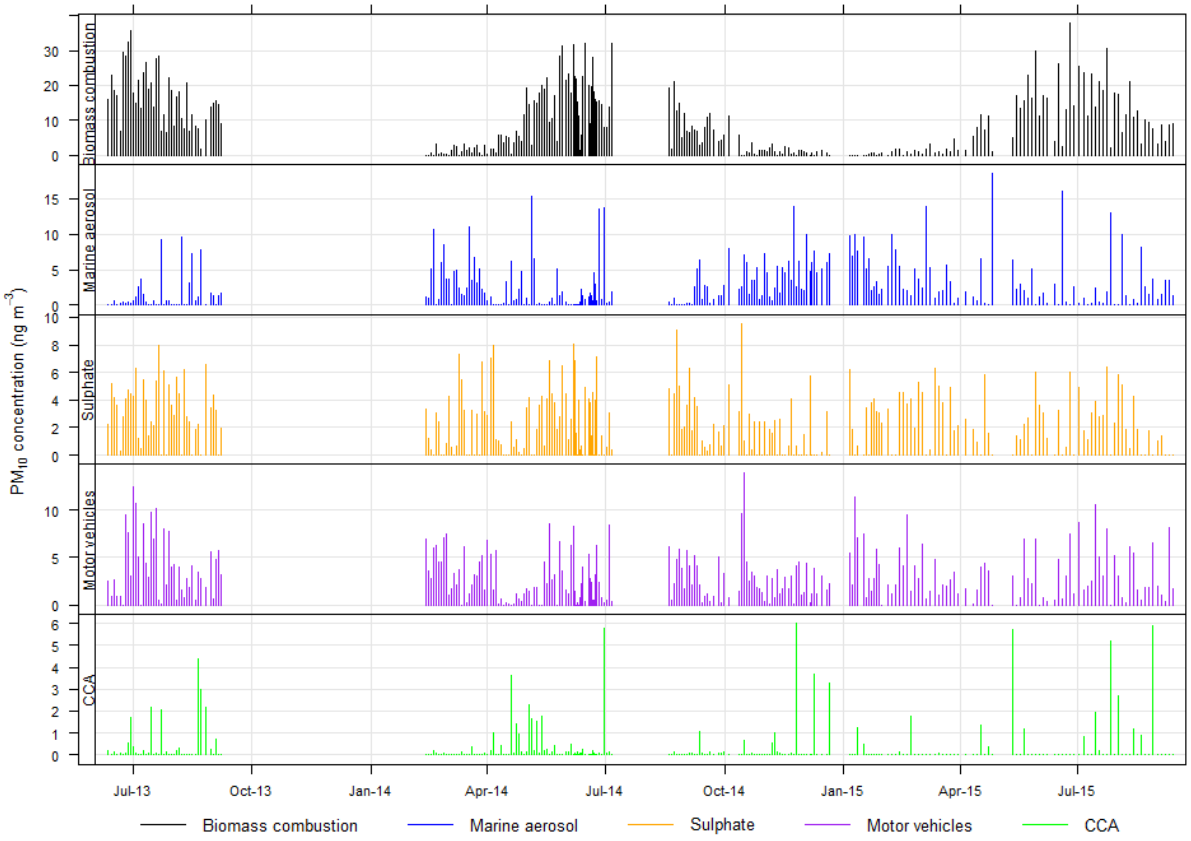

Figure 4.6 Temporal variations in relative source contributions to PM_{10} mass.

4.3.1 Seasonal variations in PM_{10} sources

The dominant source of PM_{10} from May to September (late Autumn/Winter/early Spring) in Richmond was biomass combustion associated with solid fuel fire emissions for domestic heating. Some seasonality was apparent in the marine aerosol source, which peaked during spring and summer when wind speeds tend to increase. Otherwise, little seasonality was apparent in the motor vehicle, secondary sulphate and CCA sources. Figure 4.7 and Figure 4.8 present average monthly PM_{10} concentrations and source contributions, respectively.

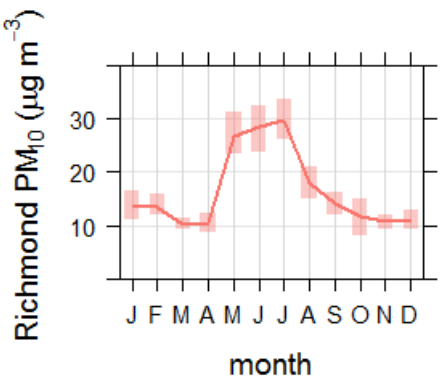

Figure 4.7 Average monthly PM_{10} concentrations in Richmond. Shaded areas represent the 95% confidence intervals.

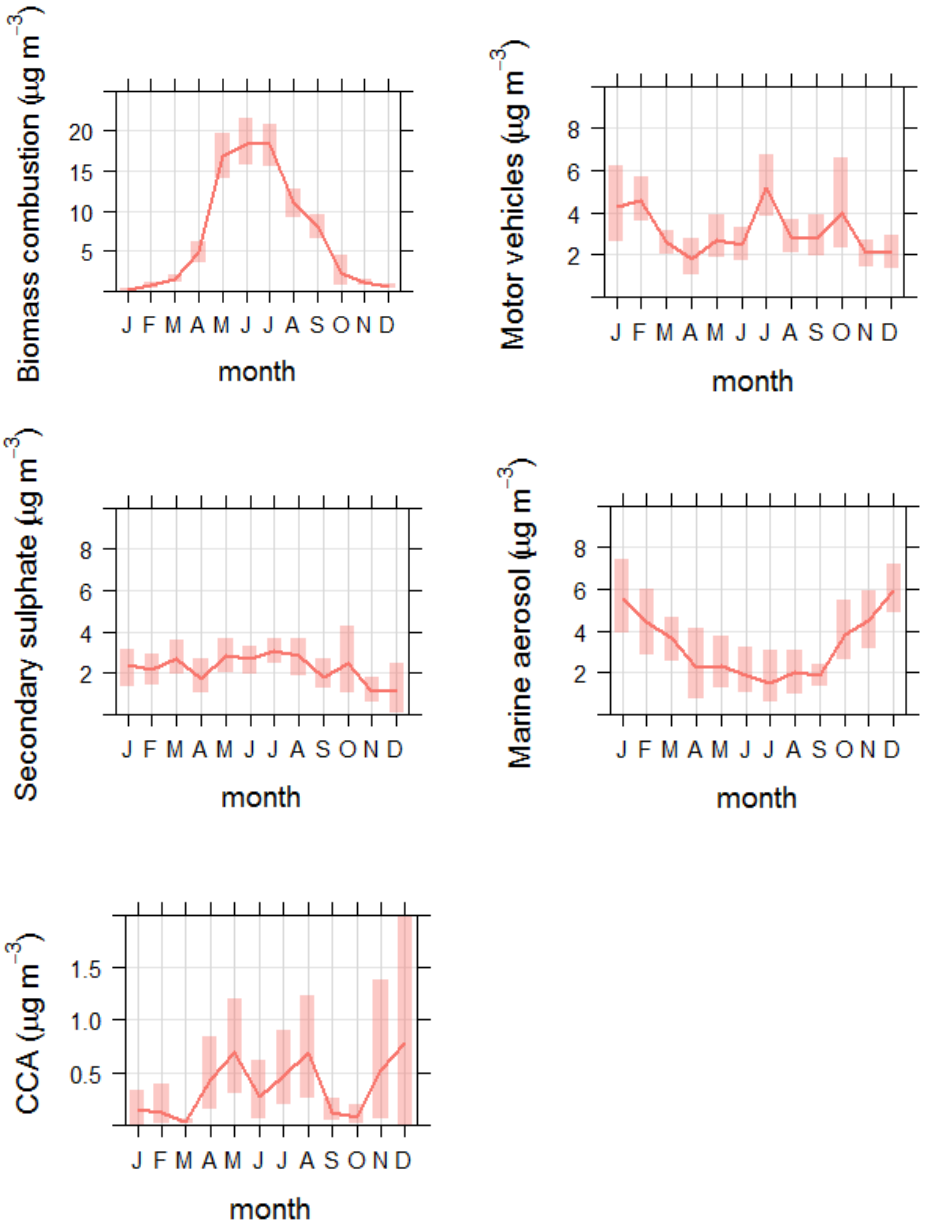

Figure 4.8 Average monthly source contributions to PM_{10} in Richmond. Shaded areas represent the 95% confidence intervals.

4.3.2 Daily variations in PM_{10} sources in Richmond

Source contributions to PM_{10} concentrations were analysed by day of the week to investigate any potential weekday/weekend variations. Figure 4.9 presents PM_{10} concentration variations by day of the week. It is evident that PM_{10} concentrations were not statistically different day-to-day, and no weekday/weekend difference was apparent. However, analysis of source contributions revealed that the motor vehicle source contributions were significantly lower on weekends than weekdays (Figure 4.10), and is likely to be indicative of lower traffic densities during the weekend than weekdays associated with normal working week and commuter behaviour.

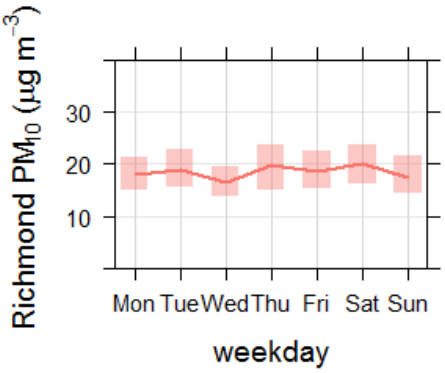

Figure 4.9 Variation in PM_{10} concentrations in Richmond by day of the week. Shaded areas represent the 95% confidence intervals.

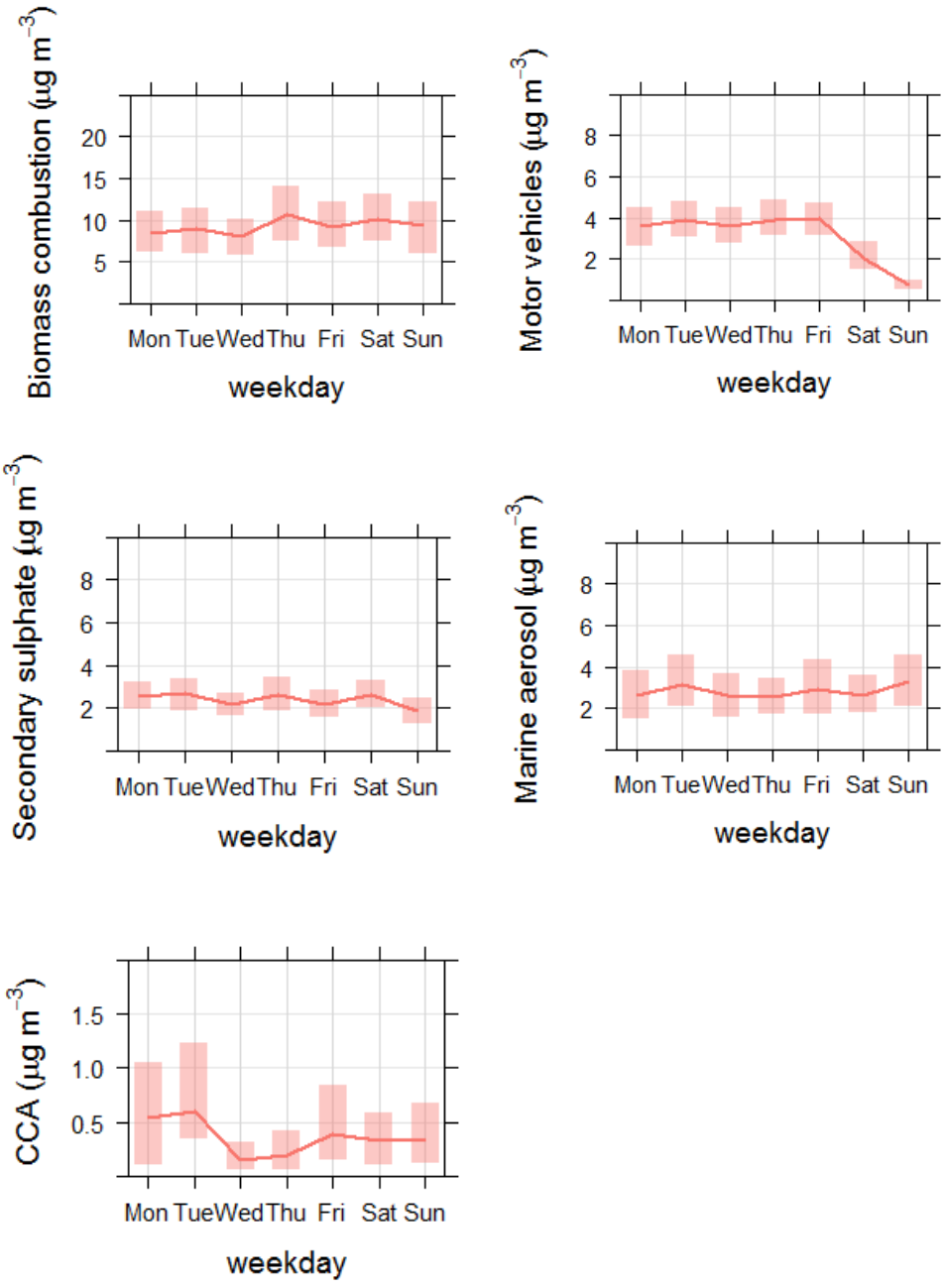

Figure 4.10 Variation in source contributions to PM_{10} in Richmond by day of the week. Shaded areas represent the 95% confidence intervals.

4.4 VARIATIONS IN PM_{10} SOURCE CONTRIBUTIONS IN RICHMOND WITH WIND DIRECTION

Bivariate polar plots using the source contributions to PM_{10} were produced using R statistical software and the openair package (Team 2011, Carslaw 2012, Carslaw and Ropkins 2012). Using bivariate polar plots, source contributions can be shown as a function of both wind speed and direction, providing invaluable information about potential source regions and how pollution from a specific source builds up. To produce the polar plots, wind speeds and directions were vector averaged using functions available in openair. A full description of the vector averaging process can be found in Carslaw (2012). The statistic = "weighted.mean" has been used here because it provides an indication of the concentration × frequency of occurrence and will highlight the wind speed/direction conditions that dominate the overall mean contribution of the source. Because of the smoothing involved, the colour scale is only

to provide an indication of overall pattern and should not be interpreted in concentration units e.g. for statistic = "weighted.mean", where the bin mean is multiplied by the bin frequency and divided by the total frequency. Note that the meteorological data used for the polar plot analysis was that supplied by TDC from their Queen Street site.

4.4.1 Biomass combustion

Biomass combustion source contributions to PM_{10} are considered to be primarily from domestic solid fuel fire emissions. Figure 4.11 presents a bivariate polar plot of biomass combustion contributions to PM_{10}. Figure 4.11 shows that peak biomass combustion contributions occurred under low wind speeds from the southwest. This indicates that katabatic flows under cold and calm anticyclonic synoptic meteorological conditions coupled with domestic fire emissions and poor dispersion were likely responsible for elevated particle concentrations, similar to previous results in other New Zealand locations (Ancelet, Davy et al. 2012, Ancelet, Davy et al. 2013). Such meteorological conditions can reasonably be anticipated one or two days ahead of time so that it can be used as a predictor of high concentrations of particulate matter pollution due to domestic fires or to issue warnings of an air pollution risk.

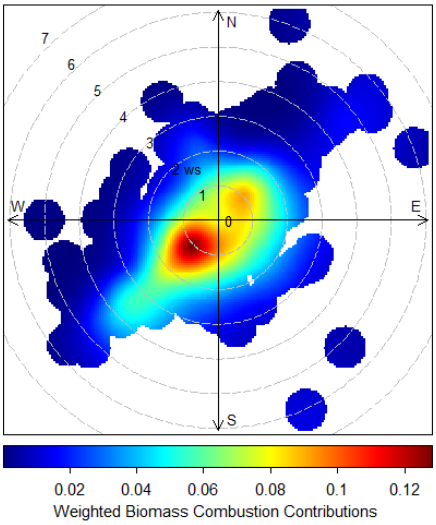

Figure 4.11 Polar plot of biomass combustion contributions to PM_{10} concentrations. The radial dimensions indicate the wind speed in 1 m s^{-1} increments and the color contours indicate the average contribution to each wind direction/speed bin.

4.4.2 Marine aerosol

Marine aerosol contributions in Richmond peaked under high wind speeds especially during summer from the northeast (Figure 4.12). The most likely sources of marine aerosol were the Tasman Sea and Southern Ocean.

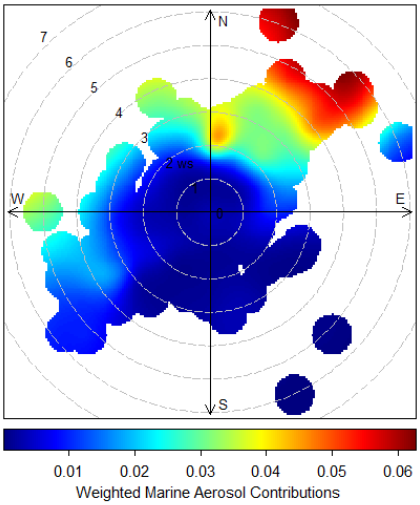

Figure 4.12 Polar plot of marine aerosol contributions to PM_{10} concentrations. The radial dimensions indicate the wind speed in 1 m s^{-1} increments and the color contours indicate the average contribution to each wind direction/speed bin.

4.4.3 Secondary sulphate

Secondary sulphate contributions in Richmond originated from north of the monitoring site (Figure 4.13). It is possible that shipping emissions from the Nelson Port contributed to the secondary sulphate concentrations. However, other sources of secondary sulphate include natural emissions (marine phytoplankton and volcanic sources) and industrial emissions. Further discussion on the secondary sulphate source is provided in Section 5.1.3.

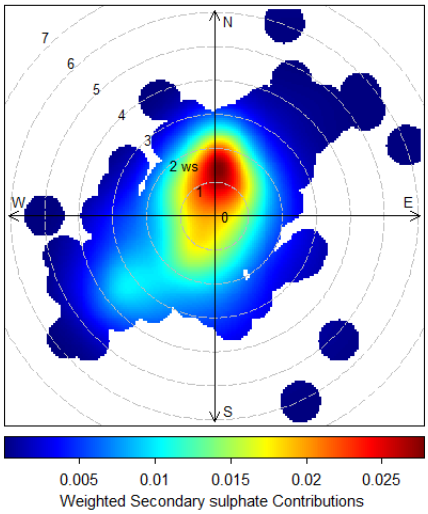

Figure 4.13 Polar plot of secondary sulphate contributions to PM_{10} concentrations. The radial dimensions indicate the wind speed in 1 m s^{-1} increments and the color contours indicate the average contribution to each wind direction/speed bin.

4.4.4 Motor vehicles

Peak motor vehicle contributions at the monitoring site occurred under winds from the north to northwest (Figure 4.14). This further supports to the assignment of the motor vehicle source (including road dust) since SH6, the main arterial route between Richmond and Nelson, is located in this sector (running southwest to northeast) relative to the monitoring site with the major component of the road (acting as a line source) to the north.

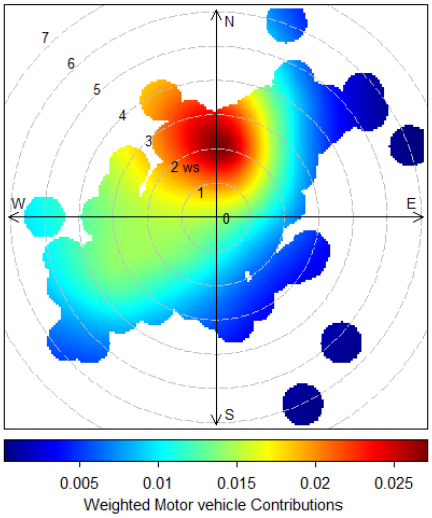

Figure 4.14 Polar plot of motor vehicle contributions to PM_{10} concentrations. The radial dimensions indicate the wind speed in 1 m s^{-1} increments and the color contours indicate the average contribution to each wind direction/speed bin.

4.4.5 CCA

Figure 4.15 shows that CCA contributions peaked under high wind speeds from the northeast. This result is interesting because if the CCA source resulted from wood combustion, it would be expected that its contributions would increase under low wind speeds. It is possible that this source originated further afield than in Richmond (e.g. Nelson), or that a local industry (or some other activity) was emitting CCA containing particles. This phenomenon highlights why, even though CCA-treated wood combustion contributes to the biomass combustion profile, a separate CCA source has been identified – the two sources are different, either in their origin or production. The origins of this source should be investigated further.

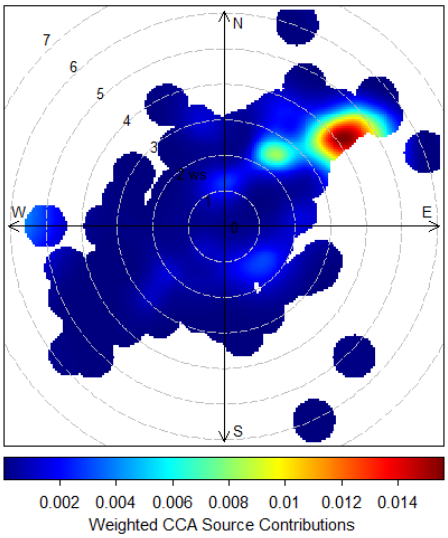

Figure 4.15 Polar plot of CCA contributions to PM_{10} concentrations. The radial dimensions indicate the wind speed in 1 m s^{-1} increments and the color contours indicate the average contribution to each wind direction/speed bin.

This page is intentionally left blank.

5.0 DISCUSSION OF THE RECEPTOR MODELING RESULTS

Monitoring of PM_{10} in Richmond shows that concentrations peak during the winter and that the NES for PM_{10} was exceeded on several occasions. Five source contributors to PM_{10} were identified from receptor modeling. The receptor modeling analysis showed that some source contributors had distinct seasonalities and that PM_{10} concentrations were primarily influenced by local emission sources.

5.1 SOURCES OF PM_{10} IN RICHMOND

5.1.1 Biomass combustion

Analysis of temporal and seasonal trends showed that PM_{10} from biomass combustion peaked during the winter (Figure 4.6 and Figure 4.8) and showed no variation between days of the week (Figure 4.10). The lack of variation between days of the week was not surprising because peak biomass combustion contributions occur under meteorological conditions conducive to the build-up of pollutants (cold, calm, anticyclonic conditions). The biomass combustion source originates from domestic wood combustion for home heating and also includes arsenic and lead in the profile, suggesting that CCA-treated and lead-painted wood is being included as fuel. It was found that the annual average arsenic concentrations for 2014 (14 ng m^{-3}) exceeded the NZAAQG (5.5 ng m^{-3} as an annual average). This study has shown that there were two sources of arsenic containing particulate matter. Table 4.2 shows that the biomass combustion source contributed 7 ng m^{-3} arsenic on average over the entire monitoring period and arsenic concentrations from biomass combustion were calculated to be 5.6 ng m^{-3} as an annual average for 2014. The use of such contaminated timber as fuel for domestic fires appears to be common throughout New Zealand including Nelson (Davy, Trompetter et al. 2010, Davy, Trompetter et al. 2011, Ancelet, Davy et al. 2012, Davy, Ancelet et al. 2012, Davy and Ancelet 2014, Davy, Ancelet et al. 2014).

Biomass combustion was identified to be responsible for peak PM_{10} concentrations, and for consequent exceedances of the NES. Further discussion on peak events is provided in Section 5.2.

5.1.2 Marine aerosol

The elemental composition for the marine aerosol source closely resembled that of seawater and the source profile is dominated by chlorine and sodium, as shown in Figure 4.2. Analysis of temporal and seasonal variations in marine aerosol showed higher concentrations during spring and summer, indicating that the generation of marine aerosol is dependent on meteorological factors, such as wind and evaporation potential. Analysis of marine aerosol contributions to PM_{10} concentrations showed distinct northeasterly directionality. Interestingly the average marine aerosol contribution to PM_{10} (2.8 µg m^{-3}) was lower than those found for Wainuiomata (5.9 µg m^{-3}) and Seaview (6.3 µg m^{-3}) in Wellington (Davy, Trompetter et al. 2008, Davy, Trompetter et al. 2009) and at six Auckland sites (6–7 µg m^{-3}) (Davy, Trompetter et al. 2009). The lower marine aerosol concentrations in Richmond may reflect a sheltering effect of the surrounding mountain ranges and somewhat calmer local meteorological conditions.

5.1.3 Secondary sulphate

The PM_{10} secondary sulphate source showed no strong seasonal pattern. Analysis of the sulphate source contributions using a polar plot showed that sulphate was transported from north of the sampling site. Sources of secondary sulphate include emissions of sulphur dioxide precursor gas from shipping activities in the Nelson Port area (Davy, Trompetter et al. 2011, Ancelet, Davy et al. 2014). Longer range sources include marine phytoplankton activity (release of dimethyl sulphide as a gaseous precursor to secondary sulphate) and potentially emissions of SO_2 gas from the Central Plateau volcanic zone (Davy, Trompetter et al. 2009). The average secondary sulphate source contribution (2.4 µg m^{-3}) to PM_{10} in Richmond was higher than for Wellington (1.2 µg m^{-3} at both Seaview and Wainuiomata) and for six Auckland sites (1.3–1.5 µg m^{-3}). Additionally, temporal variations in secondary sulphate concentrations normally demonstrate higher concentrations during summer (Davy, Trompetter et al. 2011, Davy, Ancelet et al. 2012) due the influence of solar forcing and cycles in natural source production. The Richmond data (as shown in Figure 4.8) does not show any specific seasonality suggesting that there may be some localised emission source. More work would be needed to confirm this.

5.1.4 Motor vehicles

The motor vehicle source identified is a combination of vehicular tailpipe emissions (and re-suspended soil generated by the turbulent passage of vehicles on roads, carparking areas and unsealed yards. Often in urban areas, re-entrained crustal matter on roads (i.e. road dust) is the primary source of the soil component. Further support for the anthropogenic origin of this source is that weekday contributions were significantly higher than for weekends (see Figure 4.10) indicating an association with traffic density in line with commuter behaviour. This weekday-weekend variance in concentrations was also reflected in the individual crustal matter elemental components as shown for silicon, calcium and iron. If it was a natural source (i.e. wind-blown dust) then there would be no difference between day of the week over the entire monitoring period. A bivariate polar plot (Figure 4.14) of the source contributions with wind speed and direction showed that peak concentrations occurred under winds from the north to northwest, coinciding with the location of SH6, the major local arterial roadway which runs between Richmond and Nelson.

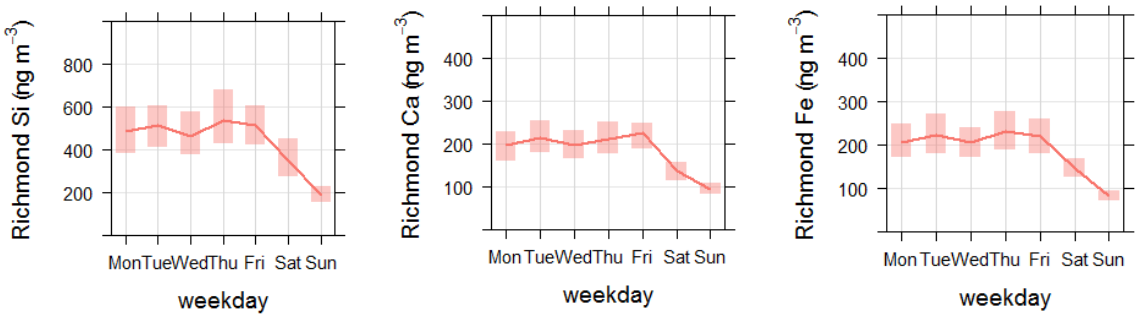

Figure 5.1 Variation in PM_{10} elemental concentrations for crustal matter components in Richmond by day of the week. Shaded areas represent the 95% confidence intervals.

5.1.5 CCA

The CCA source was intermittent, showed no seasonality or weekday/weekend differences and was a minor contributor to overall PM_{10} concentrations but was a significant contributor to average arsenic concentrations. While it could be considered evidence that locals are burning CCA-treated timber, the origins of the source are still unclear because of the lack of seasonality as opposed to normal domestic fire use during winter and the polar plot indicates that contributions increased under high wind speeds from the northeast. Table 4.2 shows that the CCA source contributed 6.4 ng m^{-3} arsenic on average over the entire monitoring period and arsenic concentrations from this source were calculated to be 6 ng m^{-3} as an annual average for 2014. When the time-series of arsenic concentrations attributed to the CCA source is compared to that of the biomass combustion source as shown in Figure 5.2, it can be seen that the biomass burning source of arsenic was consistent with winter domestic fire use. However, the CCA source of arsenic was much more intermittent with significant concentration 'spikes' when arsenic was detected and spread across both winter and summer. When coupled with the CCA polar plot presented in Figure 4.15, this pattern was more consistent with a point source of arsenic emissions originating north-east of the monitoring site (i.e. only detected at the site when source activity, wind conditions and PM_{10} sampling coincided). The other clear distinction between the two sources of arsenic was the association of copper and chromium with the CCA source which was likely to be due to the differing particulate source emission characteristics.

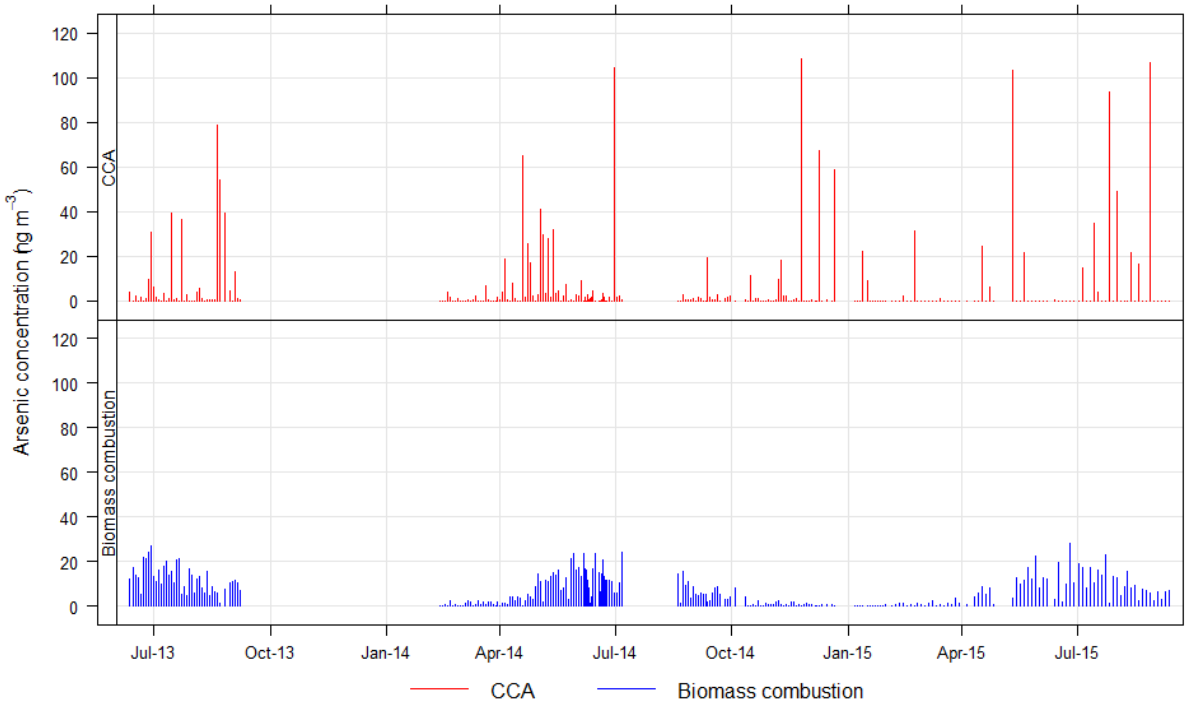

Figure 5.2 Arsenic concentrations attributed to the CCA and biomass combustion sources in Richmond.

Further work is required to identify whether these contributions are from CCA-treated timber combustion further afield, or whether there is a local industry or other activity that could be emitting CCA containing particles.

5.2 ANALYSIS OF CONTRIBUTIONS TO PM_{10} ON PEAK DAYS

For air quality management purposes, contributions from the various sources to peak PM_{10} events are of most interest. Therefore, the mass contributions of sources to all PM_{10} concentrations over 33 µg m^{-3} (the Ministry for the Environment 'Alert' level as discussed in Section 2.1) are presented in Figure 5.3. It should be noted that the concentrations presented in Figure 5.3 are those from the PMF results. To select concentrations above the 'Alert' level, actual PM_{10} concentrations measured by Tasman District Council were used.

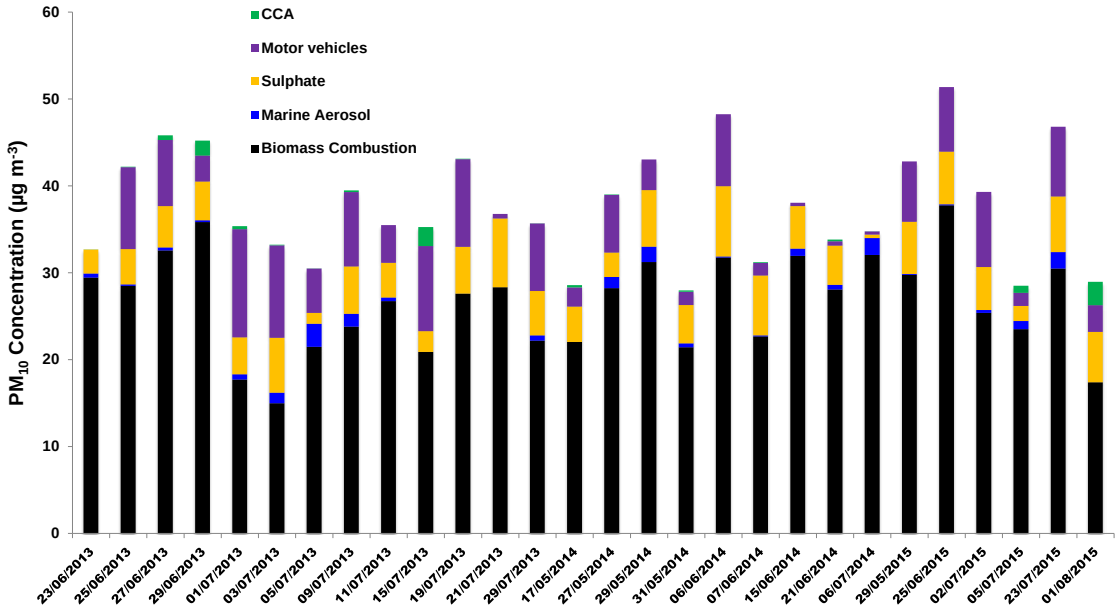

Figure 5.3 Mass contributions to peak PM_{10} events (> 33 µg m^{-3}) in Richmond.

Figure 5.3 shows that peak PM_{10} events occurred primarily during autumn and winter, and that biomass combustion was responsible for an average of 71 % of PM_{10} mass on high pollution days. On two days, biomass combustion was responsible for more than 90 % (contributing up to 92 %) of PM_{10} mass. There are several days where other particle sources (motor vehicles and sulphate) have a significant influence on PM_{10} concentrations, but none contributed sufficient PM_{10} concentrations on their own to result in an exceedance of the NES. It is likely that domestic fire emissions will continue to be primarily responsible for NES exceedances out to the 2020 full compliance date.

Furthermore, as found in other New Zealand urban areas (Davy, Ancelet et al. 2012, Ancelet, Davy et al. 2013, Ancelet, Davy et al. 2014), high pollution nights during winter dominated by biomass burning emissions most of the particulate matter is in the fine fraction ($PM_{2.5}$). It is likely that there were more days where $PM_{2.5}$ exceeded the New Zealand Ambient Air Quality Guideline (NZAAQG) compared to PM_{10} NES exceedances.

6.0 REFERENCES

Ancelet, T., P. Davy, K. and W. J. Trompetter (2013). Source apportionment of PM10 and PM2.5 in Nelson Airshed A, GNS Science Consultancy Report 2013/146.

Ancelet, T., P. K. Davy, T. Mitchell, W. J. Trompetter, A. Markwitz and D. C. Weatherburn (2012). "Identification of particulate matter sources on an hourly time-scale in a wood burning community." Environmental Science and Technology **46**(9): 4767-4774.

Ancelet, T., P. K. Davy, W. J. Trompetter, A. Markwitz and D. C. Weatherburn (2013). "Particulate matter sources on an hourly time-scale in a rural community during the winter." Journal of the Air and Waste Management Association.

Ancelet, T., P. K. Davy, W. J. Trompetter, A. Markwitz and D. C. Weatherburn (2014). "Sources and transport of particulate matter on an hourly time-scale during the winter in a New Zealand urban valley." Urban Climate.

Begum, B. A., P. K. Hopke and W. X. Zhao (2005). "Source identification of fine particles in Washington, DC, by expanded factor analysis modeling." Environ. Sci. Technol. **39**(4): 1129-1137.

Brown, S. G. and H. R. Hafner (2005). Multivariate Receptor Modelling Workbook. Research Triangle Park, NC, USEPA.

Cahill, T. A., R. A. Eldred, N. Motallebi and W. C. Malm (1989). "Indirect measurement of hydrocarbon aerosols across the United States by nonsulfate hydrogen-remaining gravimetric mass correlations." Aerosol Sci. Technol. **10**(2): 421-429.

Carslaw, D. C. (2012). The openair manual - open-source tools for analysing air pollution data. Manual for version 0.7-0, King's College London.

Carslaw, D. C. and K. Ropkins (2012). "openair - an R package for air quality data analysis." Environmental Modelling & Software **27-28**: 52-61.

Chueinta, W., P. K. Hopke and P. Paatero (2000). "Investigation of sources of atmospheric aerosol at urban and suburban residential areas in Thailand by positive matrix factorization." Atmos. Environ. **34**(20): 3319-3329.

Cohen, D., G. Taha, E. Stelcer, D. Garton and G. Box (2000). The measurement and sources of fine particle elemental carbon at several key sites in NSW over the past eight years. 15th Clean Air Conference, Sydney, Clean air Society of Australia and New Zealand.

Cohen, D. D. (1999). "Accelerator based ion beam techniques for trace element aerosol analysis." Advances in Environmental, Industrial and Process Control Technologies **1**(Elemental Analysis of Airborne Particles): 139-196.

Davy, P., K. (2007). Composition and Sources of Aerosol in the Wellington Region of New Zealand. PhD Thesis. School of Chemical and Physical Sciences. Wellington, Victoria University of Wellington**:** 429 pages.

Davy, P., K. and T. Ancelet (2014). Air particulate matter composition, sources and trends in the Whangarei Airshed, GNS Science**:** 58.

Davy, P., K., W. Trompetter and A. Markwitz (2009). Source apportionment of airborne particles at Wainuiomata, Lower Hutt. Wellington, GNS Science Client Report 2009/188.

Davy, P., K., W. Trompetter and A. Markwitz (2009). Source apportionment of airborne particles in the Auckland region: 2008 Update. Wellington, GNS Science Client Report 2009/165.

Davy, P., K., W. J. Trompetter and A. Markwitz (2007). Source apportionment of airborne particles in the Auckland region. Wellington, GNS Science Client Report 2007/314.

Davy, P., K., W. J. Trompetter and A. Markwitz (2008). Source apportionment of airborne particles at Seaview, Lower Hutt. Wellington, GNS Science Client Report 2008/160.

Davy, P. K., T. Ancelet, W. J. Trompetter and A. Markwitz (2014). Arsenic and air pollution in New Zealand. 5th International Congress on Arsenic in the Environment, As 2014, Buenos Aires, CRC Press/Balkema.

Davy, P. K., T. Ancelet, W. J. Trompetter, A. Markwitz and D. C. Weatherburn (2012). "Composition and source contributions of air particulate matter pollution in a New Zealand suburban town." Atmospheric Pollution Research **3**(1): 143-147.

Davy, P. K., W. J. Trompetter and A. Markwitz (2010). Source apportionment of PM10 at Tahunanui, Nelson, GNS Science Client Report 2010/198.

Davy, P. K., W. J. Trompetter and A. Markwitz (2011). Source apportionment of airborne particles in the Auckland region: 2010 Analysis. Wellington, GNS Science Client Report 2010/262.

Eberly, S. (2005). EPA PMF 1.1 User's Guide, USEPA.

Fine, P. M., G. R. Cass and B. R. Simoneit (2001). "Chemical characterization of fine particle emissions from fireplace combustion of woods grown in the northeastern United States." Environ. Sci. Technol. **35**(13): 2665-2675.

Hopke, P. K., Y. L. Xie and P. Paatero (1999). "Mixed multiway analysis of airborne particle composition data." J. Chemomet. **13**(3-4): 343-352.

Horvath, H. (1993). "Atmospheric Light Absorption - A Review." Atmos. Environ, **27A**: 293-317.

Horvath, H. (1997). "Experimental calibration for aerosol light absorbtion measurements using the integrating plate method - Summary of the data." Aerosol Science **28**: 2885-2887.

Jacobson, M. C., H. C. Hansson, K. J. Noone and R. J. Charlson (2000). "Organic atmospheric aerosols: review and state of the science." Reviews of Geophysics **38**(2): 267-294.

Jeong, C.-H., P. K. Hopke, E. Kim and D.-W. Lee (2004). "The comparison between thermal-optical transmittance elemental carbon and Aethalometer black carbon measured at multiple monitoring sites." Atmos. Environ. **38**(31): 5193.

Kara, M., P. K. Hopke, Y. Dumanoglu, H. Altiok, T. Elbir, M. Odabasi and A. Bayram (2015). "Characterization of PM Using Multiple Site Data in a Heavily Industrialized Region of Turkey." Aerosol and Air Quality Research **15**(1): 11-+.

Khalil, M. A. K. and R. A. Rasmussen (2003). "Tracers of wood smoke." Atmospheric Environment **37**(9-10): 1211-1222.

Kim, E., P. K. Hopke and E. S. Edgerton (2003). "Source identification of Atlanta aerosol by positive matrix factorization." J. Air Waste Manage. Assoc. **53**(6): 731-739.

Kim, E., P. K. Hopke, T. V. Larson, N. N. Maykut and J. Lewtas (2004). "Factor analysis of Seattle fine particles." Aerosol Sci. Technol. **38**(7): 724-738.

Lee, E., C. K. Chan and P. Paatero (1999). "Application of positive matrix factorization in source apportionment of particulate pollutants in Hong Kong." Atmos. Environ, **33**(19): 3201-3212.

Lee, J. H., Y. Yoshida, B. J. Turpin, P. K. Hopke, R. L. Poirot, P. J. Lioy and J. C. Oxley (2002). "Identification of sources contributing to Mid-Atlantic regional aerosol." J. Air Waste Manag. Assoc. **52**(10): 1186-1205.

Malm, W. C., J. F. Sisler, D. Huffman, R. A. Eldred and T. A. Cahill (1994). "Spatial and seasonal trends in particle concentration and optical extinction in the United States." J. Geophys. Res. Atmos. **99**(D1): 1347-1370.

MfE (2002). New Zealand Ambient Air Quality Guidelines. Wellington, New Zealand Government.

Paatero, P. (1997). "Least squares formulation of robust non-negative factor analysis." Chemom. Intell. Lab. Syst. **18**: 183-194.

Paatero, P. (2000). PMF User's Guide. Helsinki, University of Helsinki.

Paatero, P. and P. K. Hopke (2002). "Utilizing wind direction and wind speed as independent variables in multilinear receptor modeling studies." Chemometrics and Intelligent Laboratory Systems **60**(1-2): 25-41.

Paatero, P. and P. K. Hopke (2003). "Discarding or downweighting high-noise variables in factor analytic models." Analytica Chimica Acta **490**(1-2): 277-289.

Paatero, P., P. K. Hopke, B. A. Begum and S. K. Biswas (2005). "A graphical diagnostic method for assessing the rotation in factor analytical models of atmospheric pollution." Atmospheric Environment **39**(1): 193-201.

Paatero, P., P. K. Hopke, X. H. Song and Z. Ramadan (2002). "Understanding and controlling rotations in factor analytic models." Chemometrics and Intelligent Laboratory Systems **60**(1-2): 253-264.

Ramadan, Z., B. Eickhout, X.-H. Song, L. M. C. Buydens and P. K. Hopke (2003). "Comparison of Positive Matrix Factorization and Multilinear Engine for the source apportionment of particulate pollutants." Chemomet. Intellig. Lab. Syst. **66**(1): 15-28.

Salma, I., X. Chi and W. Maenhaut (2004). "Elemental and organic carbon in urban canyon and background environments in Budapest, Hungary." Atmos. Environ. **38**(1): 27-36.

Scott, A. J. (2006). Source Apportionment and Chemical Characterisation of Airborne Fine Particulate Matter in Christchurch, New Zealand. PhD Thesis, University of Canterbury.

Song, X. H., A. V. Polissar and P. K. Hopke (2001). "Sources of fine particle composition in the northeastern US." Atmospheric Environment **35**(31): 5277-5286.

Team, R. D. C. (2011). R: A language and environment for statistical computing. R Foundation for Statistical Computing, Vienna, Austria.

Trompetter, W. J. (2004). Ion Beam Analysis results of air particulate filters from the Wellington Regional Council. Wellington, Geological and Nuclear Sciences Limited.

Watson, J. G., T. Zhu, J. C. Chow, J. Engelbrecht, E. M. Fujita and W. E. Wilson (2002). "Receptor modeling application framework for particle source apportionment." Chemosphere **49**(9): 1093-1136.

This page is intentionally left blank.

APPENDICES

This page is intentionally left blank.

A1.0 ANALYSIS TECHNIQUES

A1.1 X-RAY FLUORESCENCE SPECTROSCOPY (XRF)

X-ray fluorescence spectroscopy (XRF) was used to measure elemental concentrations in PM_{10} samples collected on Teflon filters in Richmond. XRF measurements in this study were carried out at the GNS Science XRF facility and the spectrometer used was a PANalytical Epsilon 5 (PANalytical, the Netherlands). The Epsilon 5 is shown in Figure A1.1. XRF is a non-destructive and relatively rapid method for the elemental analysis of particulate matter samples.

Figure A1.1 The PANalytical Epsilon 5 spectrometer.

XRF is based on the measurement of characteristic X-rays produced by the ejection of an inner shell electron from an atom in the sample, creating a vacancy in the inner atomic shell. A higher energy electron then drops into the lower energy orbital and releases a fluorescent X-ray to remove excess energy (Watson et al., 1999 and references therein). The energy of the released X-ray is characteristic of the emitting element and the area of the fluorescent X-ray peak (intensity of the peak) is proportional to the number of emitting atoms in the sample. From the intensity it is possible to calculate a specific element's concentration by direct comparison with standards.

To eject inner shell electrons from atoms in a sample, XRF spectrometer at GNS Science uses a 100 kV Sc/W X-ray tube. The 100 kV X-rays produced by this tube are able to provide elemental information for elements from Na–U. Unlike ion beam analysis techniques, which

are similar to XRF, the PANalytical Epsilon 5 is able to use characteristic K-lines produced by each element for quantification. This is crucial for optimising limits of detection because K-lines have higher intensities and are located in less crowded regions of the X-ray spectrum. The X-rays emitted by the sample are detected using a high performance Ge detector, which further improves the detection limits. Figure A1.2 presents a sample X-ray spectrum.

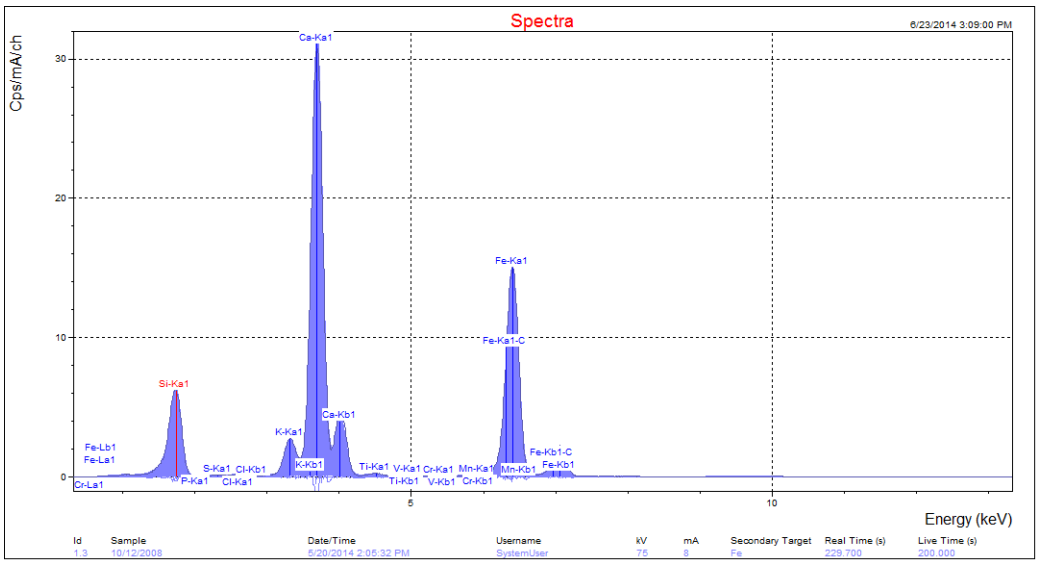

Figure A1.2 Example X-ray spectrum from a PM_{10} sample.

In this study, calibration standards for each of the elements of interest were analysed prior to the samples being run. Once the calibration standards were analysed, spectral deconvolutions were performed using PANalytical software to correct for line overlaps and ensure that the spectra were accurately fit. Calibration curves for each element of interest were produced and used to determine the elemental concentrations from the Richmond samples. A NIST reference sample was also analysed to ensure that the results obtained were robust and accurate.

References

Watson, J. G., Chow, J. C., Frazier, C. A., 1999. X-ray Fluorescence Analysis of Ambient Air Samples, in *Advances in Environmental, Industrial and Process Control Technologies* 1, 139–196.

A1.2 BLACK CARBON MEASUREMENTS

Black carbon (BC) has been studied extensively, but it is still not clear to what degree it is elemental carbon (EC (or graphitic) C(0)) or high molecular weight refractory weight organic species or a combination of both (Jacobson, Hansson et al. 2000). Current literature suggests that BC is likely a combination of both, and that for combustion sources such as petrol and diesel fuelled vehicles and biomass combustion (wood burning, coal burning), EC and organic carbon compounds (OC) are the principle aerosol components emitted (Jacobson, Hansson et al. 2000, Fine, Cass et al. 2001, Watson, Zhu et al. 2002, Salma, Chi et al. 2004).

Determination of carbon (soot) on filters was performed by light reflection to provide the BC concentration. The absorption and reflection of visible light on particles in the atmosphere or collected on filters is dependent on the particle concentration, density, refractive index and size. For atmospheric particles, BC is the most highly absorbing component in the visible light spectrum with very much smaller components coming from soils, sulphates and nitrate (Horvath 1993, Horvath 1997). Hence, to the first order it can be assumed that all the absorption on atmospheric filters is due to BC. The main sources of atmospheric BC are anthropogenic combustion sources and include biomass burning, motor vehicles and industrial emissions (Cohen, Taha et al. 2000). Cohen and co-workers found that BC is typically 10 – 40 % of the fine mass ($PM_{2.5}$) fraction in many urban areas of Australia.

When measuring BC by light reflection/transmission, light from a light source is transmitted through a filter onto a photocell. The amount of light absorption is proportional to the amount of black carbon present and provides a value that is a measure of the black carbon on the filter. Conversion of the absorbance value to an atmospheric concentration value of BC requires the use of an empirically derived equation (Cohen, Taha et al. 2000):

$$BC\ (\mu g\ cm^{-2}) = (100/2(F\varepsilon))\ \ln[R_0/R] \qquad (A1.1)$$

where:

ε is the mass absorbent coefficient for BC ($m^2\ g^{-1}$) at a given wavelength;

F is a correction factor to account for other absorbing factors such as sulphates, nitrates, shadowing and filter loading. These effects are generally assumed to be negligible and F is set at 1.00;

R_0, R are the pre- and post-reflection intensity measurements, respectively.

Black carbon was measured at GNS Science using the M43D Digital Smoke Stain Reflectometer. The following equation (from Willy Maenhaut, Institute for Nuclear Sciences, University of Gent Proeftuinstraat 86, B-9000 GENT, Belgium) was used for obtaining BC from reflectance measurements on Nucleopore polycarbonate filters or Pall Life Sciences Teflon filters:

$$BC\ (\mu g\ cm^{-2}) = [1000 \times LOG(R_{blank}/R_{sample}) + 2.39] / 45.8 \qquad (A1.2)$$

where:

R_{blank}: the average reflectance for a series of blank filters; R_{blank} is close (but not identical) to 100. GNS always use the same blank filter for adjusting to 100.

R_{sample}: the reflectance for a filter sample (normally lower than 100).

With: 2.39 and 45.8 constants derived using a series of 100 Nuclepore polycarbonate filter samples which served as secondary standards; the BC loading (in µg cm^{-2}) for these samples had been determined by Prof. Dr. M.O. Andreae (Max Planck Institute of Chemistry, Mainz, Germany) relative to standards that were prepared by collecting burning acetylene soot on filters and determining the mass concentration gravimetrically (Trompetter 2004).

References

Cohen, D., Taha, G., Stelcer, E., Garton, D., Box, G., (2000). The measurement and sources of fine particle elemental carbon at several key sites in NSW over the past eight years. *15th Clean Air Conference*, Clean air Society of Australia and New Zealand, Sydney

Horvath, H., 1993. Atmospheric Light Absorption - A Review. Atmos. Environ, 27A, 293-317.

Horvath, H., 1997. Experimental calibration for aerosol light absorbtion measurements using the integrating plate method - Summary of the data. Aerosol Science 28, 2885-2887.

Fine, P.M., Cass, G.R., Simoneit, B.R., 2001. Chemical characterization of fine particle emissions from fireplace combustion of woods grown in the northeastern United States. Environ. Sci. Technol. 35, 2665-2675.

Jacobson, M.C., Hansson, H.C., Noone, K.J., Charlson, R.J., 2000. Organic atmospheric aerosols: review and state of the science. Reviews of Geophysics 38, 267-294.

Salma, I., Chi, X., Maenhaut, W., 2004. Elemental and organic carbon in urban canyon and background environments in Budapest, Hungary. Atmos. Environ. 38, 27-36.

Trompetter, W.J., (2004). Ion Beam Analysis results of air particulate filters from the Wellington Regional Council. Geological and Nuclear Sciences Limited, Wellington

Watson, J.G., Zhu, T., Chow, J.C., Engelbrecht, J., Fujita, E.M., Wilson, W.E., 2002. Receptor modeling application framework for particle source apportionment. Chemosphere 49, 1093-1136.

A1.3 POSITIVE MATRIX FACTORIZATION

Positive matrix factorisation (PMF) is a linear least-squares approach to factor analysis and was designed to overcome the receptor modeling problems associated with techniques like principal components analysis (PCA) (Paatero, Hopke et al. 2005). With PMF, sources are constrained to have non-negative species concentrations, no sample can have a negative source contribution and error estimates for each observed data point are used as point-by-point weights. This feature is a distinct advantage, in that it can accommodate missing and below detection limit data that is a common feature of environmental monitoring results (Song, Polissar et al. 2001). In fact, the signal to noise ratio for an individual elemental measurement can have a significant influence on a receptor model and modeling results. For the weakest (closest to detection limit) species, the variance may be entirely from noise (Paatero and Hopke 2002). Paatero and Hopke strongly suggest down-weighting or discarding noisy variables that are always below their detection limit or species that have a lot of error in their measurements relative to the magnitude of their concentrations (Paatero and Hopke 2003). The distinct advantage of PMF is that mass concentrations can be included in the model and the results are directly interpretable as mass contributions from each factor (source).

A1.3.1 PMF model outline

The mathematical basis for PMF is described in detail by Paatero (Paatero 1997, Paatero 2000). Briefly, PMF uses a weighted least-squares fit with the known error estimates of measured elemental concentrations used to derive the weights. In matrix notation this is indicated as:

$$X = GF + E \tag{A1.3}$$

where:

X is the known *n* x *m* matrix of *m* measured elemental species in *n* samples;

G is an *n* x *p* matrix of source contributions to the samples;

F is a *p* x *m* matrix of source compositions (source profiles).

E is a residual matrix – the difference between measurement *X* and model *Y.*

E can be defined as a function of factors *G* and *F*:

$$e_{ij} = x_{ij} - y_{ij} = x_{ij} - \sum_{k=1}^{p} g_{ik} f_{kj} \tag{A1.4}$$

where:

$i = 1,\ldots\ldots,n$ elements

$j = 1,\ldots\ldots,m$ samples

$k = 1,\ldots\ldots,p$ sources

PMF constrains all elements of *G* and *F* to be non-negative, meaning that elements cannot have negative concentrations and samples cannot have negative source contributions as in real space. The task of PMF is to minimise the function *Q* such that:

$$Q(E) = \sum_{i=1}^{n} \sum_{j=1}^{m} (e_{ik} / \sigma_{kj})^2 \quad \text{(A1.5)}$$

where σ_{ij} is the error estimate for x_{ij}. Another advantage of PMF is the ability to handle extreme values typical of air pollutant concentrations as well as true outliers that would normally skew PCA. In either case, such high values would have significant influence on the solution (commonly referred to as leverage). PMF has been successfully applied to receptor modeling studies in a number of countries around the world (Hopke, Xie et al. 1999, Lee, Chan et al. 1999, Chueinta, Hopke et al. 2000, Song, Polissar et al. 2001, Lee, Yoshida et al. 2002, Kim, Hopke et al. 2003, Jeong, Hopke et al. 2004, Kim, Hopke et al. 2004, Begum, Hopke et al. 2005) including New Zealand (Scott 2006, Davy 2007, Davy, Trompetter et al. 2007, Davy, Trompetter et al. 2008, Davy, Trompetter et al. 2009, Davy, Trompetter et al. 2009, Ancelet, Davy et al. 2012).

A1.3.2 PMF model used

Two programs have been written to implement different algorithms for solving the least squares PMF problem, these are PMF2 and EPAPMF, which incorporates the Multilinear Engine (ME-2) (Hopke, Xie et al. 1999, Ramadan, Eickhout et al. 2003). In effect, the EPAPMF program provides a more flexible framework than PMF2 for controlling the solutions of the factor analysis with the ability of imposing explicit external constraints.

This study used EPAPMF 5.0 (version 14.1.3), which incorporates a graphical user interface (GUI) based on the ME-2 program. Both PMF2 and EPAPMF programs can be operated in a robust mode, meaning that “outliers” are not allowed to overly influence the fitting of the contributions and profiles (Eberly 2005). The user specifies two input files, one file with the concentrations and one with the uncertainties associated with those concentrations. The methodology for developing an uncertainty matrix associated with the elemental concentrations for this work is discussed in Section A1.4.2.

A1.3.3 PMF model inputs

The PMF programs provide the user with a number of choices in model parameters that can influence the final solution. Two parameters, the ‘signal-to-noise ratio’ and the ‘species category’ are of particular importance and are described below.

Signal-to-noise ratio - this is a useful diagnostic statistic estimated from the input data and uncertainty files using the following calculation:

$$(1/2) \sqrt{\sum_{i=1}^{n} (x_{ij})^2 / \sum_{i=1}^{n} (\sigma_{ij})^2} \quad \text{(A1.6)}$$

Where x_{ij} and σ_{ij} are the concentration and uncertainty, respectively, of the i^{th} element in the j^{th} sample. Smaller signal-to-noise ratios indicate that the measured elemental concentrations are generally near the detection limit and the user should consider whether to include that

species in the receptor model or at least strongly down-weight it (Paatero and Hopke 2003). The signal-to-noise ratios (S/N ratio) for each element are reported alongside other statistical data in the results section.

Species category - this enables the user to specify whether the elemental species should be considered:

- Strong – whereby the element is generally present in concentrations well above the LOD (high signal to noise ratio) and the uncertainty matrix is a reasonable representation of the errors.
- Weak – where the element may be present in concentrations near the LOD (low signal to noise ratio); there is doubt about some of the measurements and/or the error estimates; or the elemental species is only detected some of the time. If 'Weak' is chosen EPA.PMF increases the user-provided uncertainties for that variable by a factor of 3.
- Bad – that variable is excluded from the model run.

For this work, an element with concentrations at least 3 times above the LOD, a high signal to noise ratio (> 2) and present in all samples was considered 'Strong'. Variables were labelled as weak if their concentrations were generally low, had a low signal to noise ratio, were only present in a few samples or there was a lower level of confidence in their measurement. Mass concentration gravimetric measurements and BC were also down weighted as 'Weak' because their concentrations are generally several orders of magnitude above other species, which can have the tendency to 'pull' the model. Paatero and Hopke recommend that such variables be down weighted and that it doesn't particularly affect the model fitting if those variables are from real sources (Paatero and Hopke 2003). What does affect the model severely is if a dubious variable is over-weighted. Elements that had a low signal to noise ratio (< 0.2), or had mostly missing (zero) values, or were doubtful for any reason, were labelled as 'Bad' and were subsequently not included in the analyses.

If the model is appropriate for the data and if the uncertainties specified are truly reflective of the uncertainties in the data, then Q (according to Eberly) should be approximately equal to the number of data points in the concentration data set (Eberly 2005):

$$\textit{Theoretical } Q = \#\textit{ samples } \mathbf{x} \#\textit{ species measured} \tag{A1.7}$$

However, a slightly different approach to calculating the Theoretical Q value was recommended by (Brown and Hafner 2005), which takes into account the degrees of freedom in the PMF model and the additional constraints in place for each model run. This theoretical Q calculation Q_{th} is given as:

$$Q_{th} = (\#\textit{ samples } \mathbf{x} \#\textit{ good species}) + [(\#\textit{ samples } \mathbf{x} \#\textit{ weak species})/3] - (\#\textit{ samples } \mathbf{x} \textit{ factors estimated}) \tag{A1.8}$$

Both approaches have been taken into account for this study and it is likely that the actual value lies somewhere between the two.

In PMF, it is assumed that only the x_{ij}'s are known and that the goal is to estimate the contributions (g_{ik}) and the factors (or profiles) (f_{kj}). It is assumed that the contributions and mass fractions are all non-negative, hence the "constrained" part of the least-squares. Additionally, EPAPMF allows the user to say how much uncertainty there is in each x_{ij}. Species-days with lots of uncertainty are not allowed to influence the estimation of the

contributions and profiles as much as those with small uncertainty, hence the “weighted” part of the least squares and the advantage of this approach over PCA.

Diagnostic outputs from the PMF models were used to guide the appropriateness of the number of factors generated and how well the receptor modelling was accounting for the input data. Where necessary, initial solutions have been ‘rotated’ to provide a better separation of factors (sources) that were considered physically reasonable (Paatero, Hopke et al. 2002). Each PMF model run reported in this study is accompanied by the modelling statistics along with comments where appropriate.

A1.4 DATASET QUALITY ASSURANCE

Quality assurance of sample elemental datasets is vital so that any dubious samples, measurements and outliers are removed as these will invariably affect the results of receptor modelling. In general, the larger the dataset used for receptor modelling, the more robust the analysis. The following sections describe the methodology used to check data integrity and provide a quality assurance process that ensured that the data being used in subsequent factor analysis was as robust as possible.

A1.4.1 Mass reconstruction and mass closure

Once the sample analysis for the range of analytes has been carried out, it is important to check that total measured mass does not exceed gravimetric mass (Cohen 1999). Ideally, when elemental analysis and organic compound analysis has been undertaken on the same sample one can reconstruct the mass using the following general equation for ambient samples as a first approximation (Cahill, Eldred et al. 1989, Malm, Sisler et al. 1994, Cohen 1999):

$$\text{Reconstructed mass} = [\text{Soil}] + [\text{BC}] + [\text{Smoke}] + [\text{Sulphate}] + [\text{Seasalt}] \quad \text{(A1.9)}$$

where:

$[\text{Soil}] = 2.20[\text{Al}] + 2.49[\text{Si}] + 1.63[\text{Ca}] + 2.42[\text{Fe}] + 1.94[\text{Ti}]$

[BC] = Concentration of black carbon (soot)

$[\text{Smoke}] = [\text{K}] - 0.6[\text{Fe}]$

$[\text{Seasalt}] = 2.54[\text{Na}]$

$[\text{Sulphate}] = 4.125[\text{S}]$

The reconstructed mass (RCM) is based on the fact that the six composite variables or ‘pseudo’ sources given in equation A1.9 are generally the major contributors to fine and coarse particle mass and are based on geochemical principles and constraints. The [Soil] factor contains elements predominantly found crustal matter (Al, Si, Ca, Fe, Ti) and includes a multiplier to correct for oxygen content and an additional multiplier of 1.16 to correct for the fact that three major oxide contributors (MgO, K_2O, Na_2O) carbonate and bound water are excluded from the equation.

[BC] is the concentration of black carbon, measured in this case by light reflectance/absorbance. [Smoke] represents K not included as part of crustal matter and tends to be an indicator of biomass burning.

[Seasalt] represents the marine aerosol contribution and assumes that the NaCl weight is 2.54 times the Na concentration. Na is used as it is well known that Cl can be volatilised from aerosol or from filters in the presence of acidic aerosol, particularly in the fine fraction via the following reactions (Lee, Chan et al. 1999):

$$NaCl(p) + HNO_3(ag) \rightarrow NaNO_3(p) + HCL(g) \quad \text{(A1.10)}$$

$$2NaCl(p) + H_2SO_4(ag) \rightarrow Na_2SO_4(p) + 2HCL(g) \quad \text{(A1.11)}$$

Alternatively, where Cl loss is likely to be minimal, such as in the coarse fraction or for both size fractions near coastal locations and relatively clean air in the absence of acid aerosol, then the reciprocal calculation of [Seasalt] = 1.65[Cl] can be substituted, particularly where Na concentrations are uncertain.

Most fine sulphate particles are the result of oxidation of SO_2 gas to sulphate particles in the atmosphere (Malm, Sisler et al. 1994). It is assumed that sulphate is present in fully neutralised form as ammonium sulphate. [Sulphate] therefore represents the ammonium sulphate contribution to aerosol mass with the multiplicative factor of 4.125[S] to account for ammonium ion and oxygen mass (i.e. $(NH_4)_2SO_4$ = ((14 + 4)2 + 32 + (16x4)/32)).

Additionally, the sulphate component not associated with seasalt can be calculated from equation A1.13 (Cohen 1999):

$$\text{Non-seasalt sulphate (NSS-Sulphate)} = 4.125\ ([S_{tot}] - 0.0543[Cl]) \qquad \text{(A1.12)}$$

Where the sulphur concentrations contributed by seasalt are inferred from the chlorine concentrations, i.e. [S/Cl]seasalt = 0.0543 and the factor of 4.125 assumes that the sulphate has been fully neutralised and is generally present as $(NH_4)_2SO_4$ (Cahill, Eldred *et al*. 1990; Malm, Sisler *et al*. 1994; Cohen 1999).

The RCM and mass closure calculations using the pseudo-source and pseudo-element approach are a useful way to examine initial relationships in the data and how the measured mass of species in samples compares to gravimetric mass. Note that some scatter is possible because not all aerosols are necessarily measured and accounted for, such as all OC, ammonium species, nitrates and unbound water.

As a quality assurance mechanism, those samples for which RCM exceeded gravimetric mass or where gravimetric mass was significantly higher than RCM were examined closely to assess gravimetric mass and XRF data. Where there was significant doubt either way, those samples were excluded from the receptor modeling analysis. The reconstructed mass calculations and pseudo source estimations are presented in the appendices at the end of this report.

A1.4.2 Dataset preparation

Careful preparation of a dataset is required because serious errors in data analysis and receptor modeling results can be caused by erroneous individual data values. The general methodology followed for dataset preparation was as recommended by (Brown and Hafner 2005). For this study, all data were checked for consistency with the following parameters:

1. Individual sample collection validation;
2. Gravimetric mass validation;
3. Analysis of RCM versus gravimetric mass to ensure RCM < gravimetric;
4. Identification of unusual values including noticeably extreme values and values that normally track with other species (e.g. Al and Si) but deviate in one or two samples. Scatter plots and time series plots were used to identify unusual values. One-off events such as fireworks displays, forest fires or vegetative burn-offs may affect a receptor model as it is forced to find a profile that matches only that day;

5. Species were included in a dataset if at least 70 % of data was above the LOD and signal-to-noise ratios were checked to ensure data had sufficient variability. Important tracers of a source where less than 70 % of data was above the LOD were included but model runs with and without the data were used to assess the effect;

In practice during data analyses, the above steps were a reiterative process of cross checking as issues were identified and corrected for, or certain data excluded and the effects of this were then studied.

The following steps were followed to produce a final dataset for use in the PMF receptor model (Brown and Hafner 2005).

Below detection limit data: For given values, the reported concentration used and the corresponding uncertainty checked to ensure it had a high value.

Missing data: Substituted with the dataset median value for that species.

Uncertainties can have a large effect on model results so that they must be carefully compiled. The effect of underestimating uncertainties can be severe, while overestimating uncertainties does not do too much harm (Paatero and Hopke 2003).

Uncertainties for data: Uncertainties for the XRF elemental data were calculated using the following equations (Kara, Hopke et al. 2015):

$\sigma_{ij} = x_{ij} + 2/3(DL_j)$ for samples below limit of detection;

$\sigma_{ij} = 0.2x_{ij} + 2/3(DLj)$; $DL_j < x_{ij} < 3DL_j$ and $\sigma_{ij} = 0.1x_{ij} + 2/3(DL_j)$; $x_{ij} > 3DL_j$: for detected values

where x_{ij} is the determined concentration for species j in the ith sample, and DL_j is the detection limit for species j.

Below detection limit data: Below detection limit data was generally provided with a high % fit error and this was used to produce an uncertainty in ng m^{-3}.

Missing data: Uncertainty was calculated as 4 × median value over the entire species dataset.

PM gravimetric mass: Uncertainty given as 4 × mass value to down-weight the variable.

Reiterative model runs were used to examine the effect of including species with high uncertainties or low concentrations. In general it was found that the initial uncertainty estimations were sufficient and that adjusting the 'additional modelling uncertainty' function accommodated any issues with modelled variables such as those with residuals outside ± 3 standard deviations.

References

Ancelet, T., Davy, P.K., Mitchell, T., Trompetter, W.J., Markwitz, A., Weatherburn, D.C., 2012. Identification of particulate matter sources on an hourly time-scale in a wood burning community. Environmental Science and Technology 46, 4767-4774.

Begum, B.A., Hopke, P.K., Zhao, W.X., 2005. Source identification of fine particles in Washington, DC, by expanded factor analysis modeling. Environ. Sci. Technol. 39, 1129-1137.

Brown, S.G., Hafner, H.R., (2005). Multivariate Receptor Modelling Workbook. USEPA, Research Triangle Park, NC

Cahill, T.A., Eldred, R.A., Motallebi, N., Malm, W.C., 1989. Indirect measurement of hydrocarbon aerosols across the United States by nonsulfate hydrogen-remaining gravimetric mass correlations. Aerosol Sci. Technol. 10, 421-429.

Chueinta, W., Hopke, P.K., Paatero, P., 2000. Investigation of sources of atmospheric aerosol at urban and suburban residential areas in Thailand by positive matrix factorization. Atmos. Environ. 34, 3319-3329.

Cohen, D.D., 1999. Accelerator based ion beam techniques for trace element aerosol analysis. Advances in Environmental, Industrial and Process Control Technologies 1, 139-196.

Davy, P., K., (2007). Composition and Sources of Aerosol in the Wellington Region of New Zealand. PhD Thesis. *School of Chemical and Physical Sciences*, Victoria University of Wellington, Wellington

Davy, P., K., Trompetter, W.J., Markwitz, A., (2007). Source apportionment of airborne particles in the Auckland region. GNS Science Client Report 2007/314, Wellington

Davy, P., K., Trompetter, W.J., Markwitz, A., (2008). Source apportionment of airborne particles at Seaview, Lower Hutt. GNS Science Client Report 2008/160, Wellington

Davy, P., K., Trompetter, W., Markwitz, A., (2009a). Source apportionment of airborne particles at Wainuiomata, Lower Hutt. GNS Science Client Report 2009/188, Wellington

Davy, P., K., Trompetter, W., Markwitz, A., (2009b). Source apportionment of airborne particles in the Auckland region: 2008 Update. GNS Science Client Report 2009/165, Wellington

Eberly, S., (2005). EPA PMF 1.1 User's Guide. USEPA

Hopke, P.K., Xie, Y.L., Paatero, P., 1999. Mixed multiway analysis of airborne particle composition data. J. Chemomet. 13, 343-352.

Jeong, C.-H., Hopke, P.K., Kim, E., Lee, D.-W., 2004. The comparison between thermal-optical transmittance elemental carbon and Aethalometer black carbon measured at multiple monitoring sites. Atmos. Environ. 38, 5193.

Kim, E., Hopke, P.K., Edgerton, E.S., 2003. Source identification of Atlanta aerosol by positive matrix factorization. J. Air Waste Manage. Assoc. 53, 731-739.

Kim, E., Hopke, P.K., Larson, T.V., Maykut, N.N., Lewtas, J., 2004. Factor analysis of Seattle fine particles. Aerosol Sci. Technol. 38, 724-738.

Lee, E., Chan, C.K., Paatero, P., 1999. Application of positive matrix factorization in source apportionment of particulate pollutants in Hong Kong. Atmos. Environ, 33, 3201-3212.

Lee, J.H., Yoshida, Y., Turpin, B.J., Hopke, P.K., Poirot, R.L., Lioy, P.J., Oxley, J.C., 2002. Identification of sources contributing to Mid-Atlantic regional aerosol. J. Air Waste Manag. Assoc. 52, 1186-1205.

Malm, W.C., Sisler, J.F., Huffman, D., Eldred, R.A., Cahill, T.A., 1994. Spatial and seasonal trends in particle concentration and optical extinction in the United States. J. Geophys. Res. Atmos. 99, 1347-1370.

Paatero, P., 1997. Least squares formulation of robust non-negative factor analysis. Chemom. Intell. Lab. Syst. 18, 183-194.

Paatero, P., (2000). PMF User's Guide. University of Helsinki, Helsinki

Paatero, P., Hopke, P.K., 2002. Utilizing wind direction and wind speed as independent variables in multilinear receptor modeling studies. Chemometrics and Intelligent Laboratory Systems 60, 25-41.

Paatero, P., Hopke, P.K., Song, X.H., Ramadan, Z., 2002. Understanding and controlling rotations in factor analytic models. Chemometrics and Intelligent Laboratory Systems 60, 253-264.

Paatero, P., Hopke, P.K., 2003. Discarding or downweighting high-noise variables in factor analytic models. Analytica Chimica Acta 490, 277-289.

Paatero, P., Hopke, P.K., Begum, B.A., Biswas, S.K., 2005. A graphical diagnostic method for assessing the rotation in factor analytical models of atmospheric pollution. Atmospheric Environment 39, 193-201.

Ramadan, Z., Eickhout, B., Song, X.-H., Buydens, L.M.C., Hopke, P.K., 2003. Comparison of Positive Matrix Factorization and Multilinear Engine for the source apportionment of particulate pollutants. Chemomet. Intellig. Lab. Syst. 66, 15-28.

Scott, A.J., (2006). Source Apportionment and Chemical Characterisation of Airborne Fine Particulate Matter in Christchurch, New Zealand. University of Canterbury, Christchurch

Song, X.H., Polissar, A.V., Hopke, P.K., 2001. Sources of fine particle composition in the northeastern US. Atmospheric Environment 35, 5277-5286.

This page is intentionally left blank.

A2.0 ELEMENTAL CORRELATION PLOT

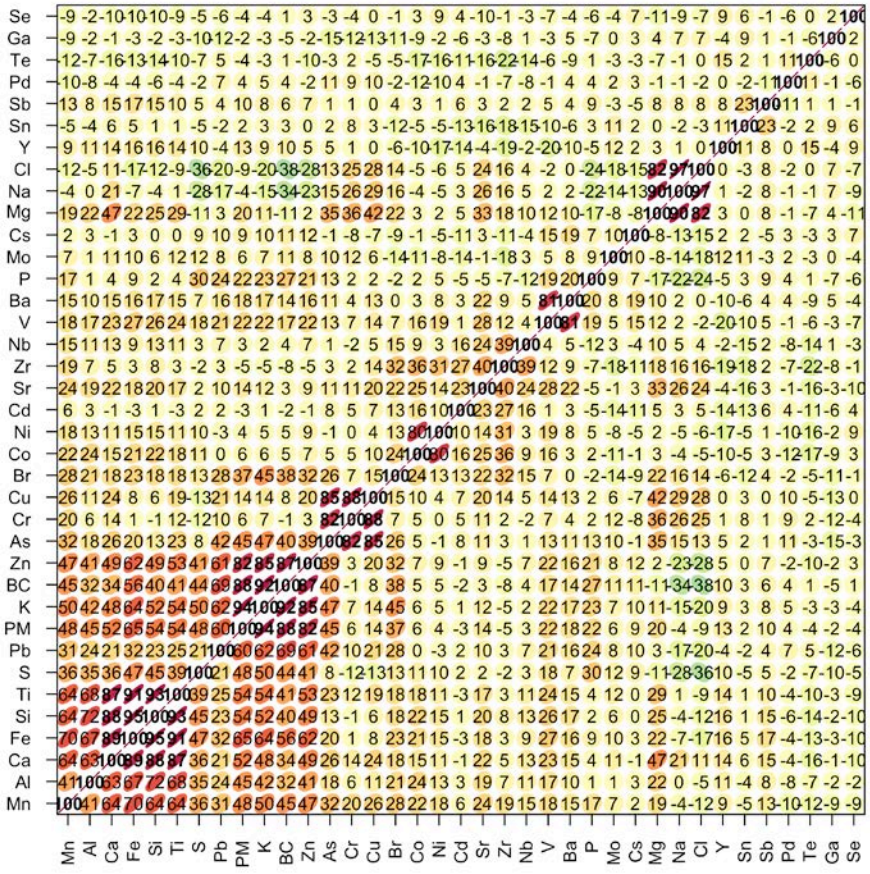

Figure A2.1 Elemental correlation plot.

www.gns.cri.nz

Principal Location

1 Fairway Drive
Avalon
PO Box 30368
Lower Hutt
New Zealand
T +64-4-570 1444
F +64-4-570 4600

Other Locations

Dunedin Research Centre
764 Cumberland Street
Private Bag 1930
Dunedin
New Zealand
T +64-3-477 4050
F +64-3-477 5232

Wairakei Research Centre
114 Karetoto Road
Wairakei
Private Bag 2000, Taupo
New Zealand
T +64-7-374 8211
F +64-7-374 8199

National Isotope Centre
30 Gracefield Road
PO Box 31312
Lower Hutt
New Zealand
T +64-4-570 1444
F +64-4-570 4657